DETERMINATION OF THE CONFORMATIONS ADOPTED BY CXCR4 AND CCR5 AT THE CELL SURFACE

By

Sunniva Yngvil Dyrhaug

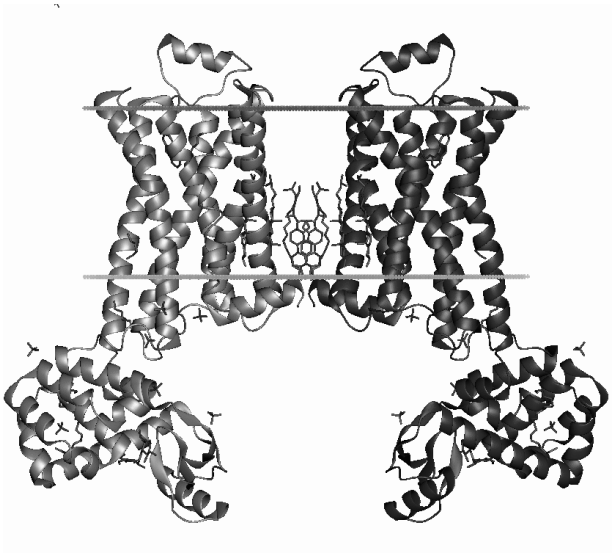

MASTER THESIS IN PHARMACY

2009 / 2010

Department of Biomedicine/Centre for Pharmacy

University of Bergen

Bergen, Norway

Department of Immunology & Oncology

National Centre for Biotechnology

Madrid, Spain

The work presented in this master thesis was carried out during the period of September 2009 to May 2010, at the laboratory of Dr. Mario Mellado, Department of Immunology and Oncology, National Centre of Biotechnology, Madrid, Spain.

ACKNOWLEDGEMENT

Firstly, I want to express my deepest gratitude and respect to Mario Mellado, for letting me join his laboratory, and for giving me the opportunity to work on this interesting project. This has been a year I will never forget, and I am deeply grateful for your encouragement, your will to always help anyway you can, your support and for having the faith in me to let me do this.

Secondly, I want to thank Laura Martinez-Muñoz, to whom I owe much of the success of this project. Without your incredible patience, positive attitude and teaching skills, I doubt this would have been possible for me to do. I am truly grateful for all the time you spent teaching me all the different techniques, finding solutions to problems occurring all the time, and providing me with positive feedback at every little opportunity. During this one year, you have taught me more about biochemistry and biotechnology than I thought was possible to learn. I will miss our conversations, turning up the music during late hours at the lab, and, I will miss someone with whom to obsess about a certain story involving certain supernatural creatures! Thank you for making this year into one of my best experiences ever.

I also want to thank To Anni Vedeler, for always showing interest in my project and keeping me in touch with the University in Bergen. Having you as my internal supervisor has been a great support for me, and I deeply appreciate your advice and efforts on making this project the best possible.

To Pili, for always showing interest in my work, for the many times you helped me lifting the cells of the saturation curves, which sometimes seemed endless, and for your efforts on the cell-cell fusion experiments. Muchísimas gracias.

To José Miguel, I will never forget my first week at CNB, trying to keep up with you teaching me the basics of cell cultivation and several experiments. It was a great start of a great year. Thank you for your constant support, your music tips, your pep talks, advice and help throughout this year.

To Damián, thank you for always supporting me in everything I do, for always listening openheartedly to my many ideas, for always speaking your mind, for always having dinner ready when I have come home late from the lab, and for caring so much.

To my mother and father. Everything I achieve, I owe to you. You are always right there behind me. Thank you is not enough, but it is the best I can say.

To my sisters and my brother, you are the best security net a little sister could ever have.

To my friends at the CNB, for making this year such a wonderful experience, filled with good memories. I will miss you.

To my fellow pharmacy students of class 05' in Norway, for staying in touch and showing support and interest in my work.

To the kitchen facility and the other parts of CNB which I have gotten to know during this year.

Thank you.

Madrid, May 2010

Sunniva Yngvil Dyrhaug

TABLE OF CONTENTS

ABBREVATIONS

BRET	Bioluminescence Resonance Energy Transfer
DNA	Deoxyribose Nucleic Acid
FRET	Fluorescence Resonance Energy Transfer
BiFC	Bimolecular Fluorescence Complementation
BSA	Bovine Serum Albumin
CFP	Cyan Fluorescent Protein
YFP	Yellow Fluorescent Protein
C- Terminus	Carboxyl Acid Terminus
CRD	Cysteine Rich Domains
DAG	Diaglycerol
DIC	Differential Interference Contrast
DMEM	Dulbecco's Modified Eagle Medium
EDTA	Ethylene Diamine Tetra Acetic Acid
FBS	Foetal Bovine Serum
FITC	Fluorescein Isothiocyanate
GPCR	G-protein coupled receptor
GRK	G-protein Receptor Kinase
GTP	Guanosine 5'triphosphate
HBSS	Hanks Balanced Salt Solution
HEPES	4-(2-hydroxyethyl)-1-piperazineethanesulfonic acid
GAP	GTPase activating protein
INF-γ	Interferon-gamma
IP3	Inositol 1,4,5-triphosphate
kDa	Kilo Dalton
MAPK	Mitogen-Activated Protein Kinase

mAb	Monoclonal Antibody
N-terminus	Amino Acid Terminus
PCR	Polymerase Chain Reaction
PBS	Phosphate Buffer Saline
PI3K	Kinase 3'Phosphatidylinositol
PIP2	Phosphatidylinositol-4,5 bisphosphate
PKC	Protein Kinase C
PLC	Phospholipase C
PTx	Pertussis Toxin
ER	Endoplasmatic Reticulum
RGS	Regulators of G-protein Signalling
SDS-PAGE	Sodium dodecyl sulphate polyacrylamide gel electrophoresis
Rpm	Revolutions per minute
PLA_2	Phospholipase A2
SPRD	Spectral Red
VFT	Venus Flytrap Domain
TNF	Tumour Necrosis Factor
TMI	Transmembrane Region 1 (1. α-helix)
TMIV	Transmembrane Region 1 (4. α-helix)

OBJECTIVES

- Generate CXCR4 and CCR5, as Cyan (CFP) and Yellow (YFP) fluorescent fusion proteins by DNA transfection of plasmids containing inserts of the corresponding cDNAs.

- Determine the expression patterns of CXCR4 CFP, CXCR4 YFP, CCR5 CFP and CCR5YFP.

- Analyze the functionality of the fusion proteins created.

- Study and determine putative homo- and hetero dimers of CXCR4 and CCR5 by Fluorescence Resonance Energy Transfer (FRET).

- Study the dynamics of the different mono-, and oligomeric forms of CXCR4 and CCR5, and determine if this affects HIV infection of cells.

SUMMARY

The chemokines and their receptors constitute many important physiological functions in the human body. The chemokine receptors belong to the family of G-protein coupled receptors, characterized by 7 α-helices penetrating the cell membrane, and are coupled to a heterotrimeric G-protein intracellularily. Discovering the phenomenon of oligomerization of the G-protein coupled receptors, increased the complexity in terms of functionality and dynamics significantly, amplifying both challenges and possibilities related to these receptors. The chemokine receptors CCR5 and CXCR4 are physiologically diverse and in addition, the two co-receptors for HIV-1. HIV-1 infects T cells through an envelope protein called gp120, which binds to CD4 on the target cell, in addition to CCR5, CXCR4 or both, depending on the strain of the virus in question. M-tropic HIV-1 gp120 enters and infects monocytes via CCR5, while the T-tropic HIV-1 p120 enters and infects lymphocytes via CXCR4. Another dual tropic strain, entering via both chemokine receptors also exists. Evidence has been published, which indicates a possible effect on HIV-1 infection related to receptor oligomerization dynamics, based on the presence of several receptors capable of forming oligomeric complexes at the cell membrane. In this project, cell functionality and receptor expression pattern of CCR5 and CXCR4 fused with a fluorescent protein (CFP or YFP) is demonstrated. In addition to this, homo- and heterodimerization between CCR5 and CXCR4 in live cells are demonstrated by the use of Fluorescence Resonance Energy Transfer (FRET). By the same technique, it is also demonstrated that CCR5 is able to decrease the apparent affinity of CXCR4 towards forming homodimers, indicating the conformation dynamics of these receptors. Finally, the importance of CXCR4 conformations in terms of T-tropic (X4) HIV-1 entry is assessed, as it is demonstrated that the presence of CCR5 at the cell surface decreases T-tropic (X4) HIV-1 infection significantly, most likely by interacting with CXCR4 and altering its conformation.

INTRODUCTION

You gain strength, courage and confidence by every experience in which you really stop to look fear in the face. You must do the thing you think you cannot do.

- *Eleanor Roosevelt (1884-1962)*

In this project, the two chemokine receptors CCR5 and CXCR4 have been studied in greater detail. The chemokine receptors, belonging to the G-protein coupled receptors, are important due to their presence in the human body and their diverse physiological function. The attention devoted to these receptors increased even more after the discovery of the phenomenon of oligomerization among the different G-protein coupled receptors. This phenomenon amplifies greatly the pharmacological diversity of these receptors, and determining the functions of the different complexes may contribute to discover new therapeutic possibilities against a wide range of pathologies.

1.1 Chemokines

Chemokines belong to a family of low molecular weight proteins (6-14 kDa), which control a wide variety of biological and pathological processes. In contrast to cytokines that share many of the same biological functions, chemokines signal through G-protein coupled receptors (GPCRs) at the cell membrane, modulating among other things immune surveillance, inflammation processes, chemotaxis, cell migration, cancer and viral infections.

Although sequence identity of the various chemokines varies from less than 20% to over 90%, they all form similar three-dimensional monomer folds, which contain a flexible N-terminal domain followed by an N- terminal loop, a three-stranded antiparallell β-sheet region and finally a C- terminal α-helix [1].

Chemokines are traditionally divided into 4 families, based on relative positioning of the first two of four highly conserved cysteine residues. Accordingly, there are; CXC, CC, C and CX_3C chemokines. The first two comprise the main families. In the CXC family members (α-chemokines), the first two cysteine residues are separated by a single non-conserved amino acid, while the first two cysteine residues are adjacent in the chemokines of the CC family (β-chemokines) [2]. The less common C family (Ω-chemokines) lacks the first and the third of the cysteine residues, while the CX_3C family (γ-chemokines), with only one member discovered at present, has three amino acids between the first two conserved cysteine residues. Nonetheless, for many years the chemokines were classified on the basis of their biological functions or the cells producing the chemokines. This resulted in a chaotic system,

and a new nomenclature regime was therefore introduced in 2000, in which every chemokine was classified into a subfamily based on the coding gene for the specific protein in the chromosome [3]. Today, nevertheless, chemokines continue to be generally classified on functional criteria, and hence, scientists commonly distinguish between homeostatic and inflammatory chemokines.

A) *B)*

Figure 1.1 A) Three dimensional structure of the monomeric (left) and the dimeric form (right) of the CC chemokine family. B) Three dimensional structure of the monomeric (left) and the dimeric form (right) of the CXC chemokine family [4].

Homeostatic chemokines are constitutively expressed in the body. They play an important role in maintaining the homeostasis of the immune system by coordinating cellular movement, such as B- and T-cell migration towards specific secondary lymphoid organs. Homeostatic chemokines are also present in other parts of the body, like skin, intestinal mucosa and lung tissue, where they contribute to migration and/or activation of different kinds of leukocytes. Examples of homeostatic chemokines are CCL19, CCL21 and CXCL12.

Inflammatory chemokines are in contrast to homeostatic chemokines inductively expressed by a variety of cells, not only within the immune system, but also by other cell types as a response to specific stimuli. The pro-inflammatory mediators (IFN-γ, pathogens, TNF, etc.) act as such stimuli, provoking the expression of these chemokines following for example an infection. The chemokines then contribute importantly to direct the cellular response towards the damaged, infected and/or inflamed area. Examples of inflammatory chemokines are CCL5, CCL3 and CXCL10.

Through mutagenesis-based studies, it has been possible to identify the binding domains and the region of the chemokines implicated in the signalling through their respective receptors

[5]. It has been demonstrated that the N-terminus plays a very important role in signalling, and that some chemokines, for instance CCL2, CCL5 and CCL9, can bind to their respective receptor, but are not capable of signalling if this region is mutated [5, 6]. For some chemokines, the activity depends on the first amino acid residue at the N-terminus. For example, erasing the 7 first amino acid residues at the extreme end of the N-terminus of CCL2 gives rise to an antagonist [6, 7]. If the serine residue at the extreme end of the N-terminus of CCL2 or CCL5 is followed by a methionine residue, chemokine antagonists are formed through peptide signalling retention. The addition of an oxi pentamino group to the extreme end of the N-terminus of CCL5 gives rise to a protein blocking HIV viral entry[8]. The affinity of CXCL12 to the receptor CXCR4 depends on the RFFESH residues (12-17 amino acid residues) [9]. Thus, the functions of the chemokines depend to a great extent on the N-terminal amino acid sequences.

1.2 Chemokine Receptors

The chemokines exert their functions through binding to their respective receptors, which belong to the heptahelical, seven transmembrane domain G-protein coupled receptor family (GPCRs). This protein superfamily is one of the most common in the proteome of mammals [10], and it is estimated that half of all modern drugs available today act through these receptors [11]. Based on sequence homology, GPCRs are classified into 5 main families;

1. Rhodopsine (701 members).
    a. α-group includes 5 subgroups; prostaglandins, receptors of neurotransmitters, melatonin receptors and MECAs.
    b. β-group includes 36 members. No subgroup classification.
    c. γ-group includes 3 subgroups. Chemokine receptors, SOG and MCH (Melanin Concentrating Hormone).
    d. δ-group includes 4 subgroups. Receptors related to the oncogene MAS, glycoprotein-related receptors, purine receptors and olfactory receptors. [12]
2. Glutamate (15 members).
3. Adhesion (24 members)
4. Frizzled (24 members)

5. Secretine (15 members) [12]

The chemokine receptors are mainly classified into a CC and CXC family, containing 11 and 7 members, respectively. The classification is based upon the four groups of ligands which they bind to (CC, CXC, CX3C and XC). In addition to these chemokine receptors, are also the non-functional (silenced) receptors D6 and DUFFY, CCX CKR receptors, and a few virally expressed receptors. The chemokine receptors consist of a single polypeptide of 350 amino acids, with a molecular mass of about 40 kDa. They are characterized by seven α-helices and penetrate the plasma membrane seven times, exposing the N-terminal and 3 loops to the extracellular site of the cell, allowing for interaction with ligands. The C-terminus and 3 loops are located on the intracellular side of the plasma membrane and are responsible for transmitting the signals via G-proteins to the interior of the cell. A motif called DRYLAIV is found exclusively in the second intracellular loop of chemokine receptors. This motif is implicated in the activation of the intracellular signalling. The binding of the ligand provokes a conformational change in this motif, such that the tyrosine139 residue originally oriented towards the interior of the receptor, turns to the exterior of the receptor, towards the cytoplasm (Fig. 1.2). This is a compulsory conformational change for signalling and the first of several, initiating the signal transmission. In fact, the mutant CCR2bY139F, lacking tyrosine139, is incapable of transmitting signals, and is therefore non-functional [13]. The so-called "silenced" receptors (D6 and DUFFY) miss the DRYLAIV motif and this is one of the reasons for their non-functionality. Currently, no tertiary structural model of the chemokine receptor exists. The only present tertiary structural models of GPCRs are the rhodopsine receptor [14], the β_2 adrenergic receptor[15] and the bacterial rhodopsine receptor, in unicellular organisms [16].

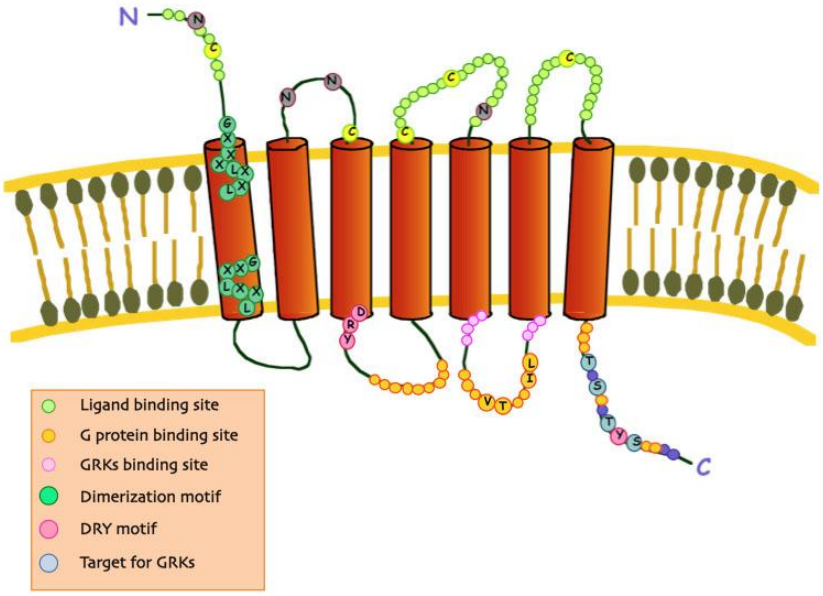

Figure 1.2: Structure of the chemokine receptor in the cell membrane. The DRYLAIV motif, the binding site of the ligand, the binding site of the G-protein as well as that of the kinesis family GRK (Section 1.2.1) are all represented in the figure. Courtesy of José Miguel Rodriguez-Frade, CNB, Madrid.

RECEPTORS	CORRESPONDING LIGANDS
CCR1	CCL3, CCL5, CCL7, CCL13, CCL14, CCL15, CCL16, CCL23
CCR2	CCL2, CCL7, CCL8, CCL13, CCL16
CCR3	CCL5, CCL7, CCL8, CCL11, CCL13, CCL15, CCL16, CCL24, CCL26, CCL28
CCR4	CCL17, CCL22
CCR5	CCL3, CCL4, CCL5, CCL8, CCL11, CCL14, CCL16
CCR6	CCL20
CCR7	CCL19, CCL21
CCR8	CCL1
CCR9	CCL25
CCR10	CCL27, CCL28
CXCR1	CXCL6, CXCL7, CXCL8
CXCR2	CXCL1, CXCL2, CXCL3, CXCL5 CXCL6, CXCL7, CXCL8
CXCR3A	CXCL9, CXCL10, CXCL11
CXCR3B	CXCL4, CXCL9, CXCL10, CXCL11
CXCR4	CXCL12
CXCR5	CXCXL13
CXCR6	CXCL16
CXCR7	CXCL12
XCR1	XCL1, XCL2
CX3CR1	CX3CL1
CCX-CKR	CCL19, CCL21, CCL25
D6	CCL2, CCL3, CCL4, CCL5, CCL7, CCL8, CCL11, CCL13, CCL14, CCL17, CCL22
DARC/Duffy	CCL2, CCL7, CCL8, CCL11, CCL13, CCL14, CCL16, CCL17, CXCL1, CXCL5, CXCL6, CXCL8, CXCL9, CXCL11, CXCL13

Table 1.1: Overview of the chemokine receptors and their corresponding ligands. Data taken from [17].

1.2.1 Receptor Activation

Most chemokine receptors activate intracellular heterotrimeric G_i proteins, and their signalling cascade is therefore blocked by Pertussis Toxin (PTx) treatment. Other G proteins have also been described to be implicated in signalling, such as G_{13} and G_q, depending on the cell type evaluated. The stable and inactive complex of the G-protein contains a GDP molecule in the α-subunit. As the G-protein is activated upon signalling through the chemokine receptor, this GDP molecule is exchanged by GTP, which in turn activates the α-subunit and results in the dissociation of the βγ-subunit. The α-subunit connects to the receptor, while the βγ- complex remains anchored to the cell membrane. Depending on the signal to be delivered, one of the subunits transmits this. As the α-subunit possesses enzymatic GTPase activity, the GTP molecule is rapidly hydrolyzed into GDP, and the G-protein is thereby turned back to its inactive state. The Gα-GDP complex has a high affinity for the βγ complex, and the three subunits are joined together again, ready for the next activation cycle (Fig. 1.3). Several proteins are implicated in the regulation of these processes. Among these are the Regulators of G-protein Signalling (RGS) which associate with the Gα-GTP complex and act as GTPase activating proteins (GAPs), accelerating the hydrolysis of the GTP molecules and thereby regulating the active state of the G-protein and the duration of the signalling. Serine-threonine kinases named GRKs are also capable of regulating the activation of the G-proteins. These proteins only phosphorylate the receptor in its active form, at the serine and threonine residues. At the same time they act as binding sites for arrestins, blocking the access of another G-protein to the receptor and thereby inhibit further signalling.

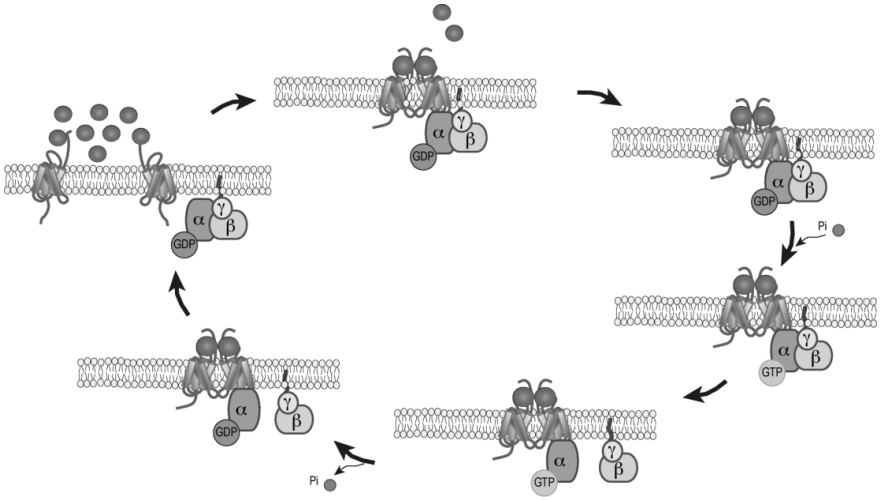

Figure 1.3: The G-protein activation cycle. Various types of G-protein α-subunits exist, and the four main groups are $G\alpha_s$, $G\alpha_i$, $G\alpha_q$ and $G\alpha_{12}$. Signalling routes depend on the type of α-subunit, but it is still not clear if the attachment of a specific G-protein to the chemokine receptor depends on of the cellular environment or simply that the other G-proteins are somehow inhibited. Courtesy of José Miguel Rodriguez-Frade, CNB, Madrid.

The G-proteins activate a broad spectre of signalling cascades, ranging from the activation of Phospholipase C (PLC), the phosphate kinesis 3'phosphoinositol (PI3K) to the Mitogen Activated Protein Kinesis (MAPK cascade) (Fig. 1.4).

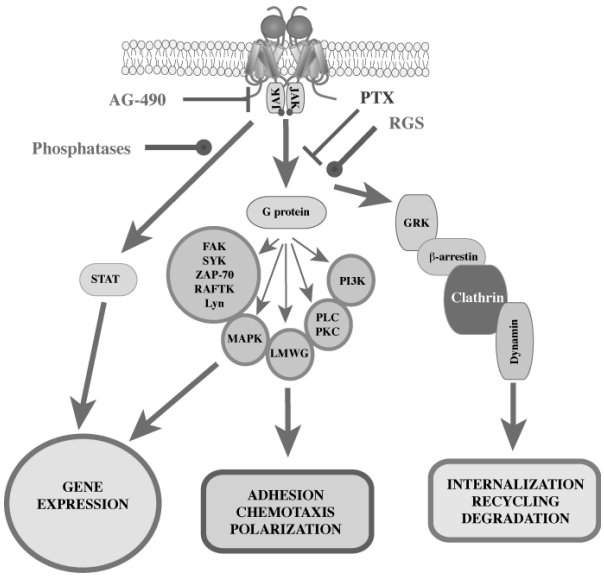

Figure 1.4 Signalling pathways activated by chemokines and chemokine receptors. Courtesy of José Miguel Rodriguez-Frade, CNB, Madrid.

Although activation of PLC is basically induced by G-proteins insensitive to PTx (ex. G_q), PLC activation produced by PTx sensitive chemokines through the βγ-complex has been described [18]. Activation of PLC promotes the hydrolysis of phosphoinsoitol bisphosphate (PIP2), forming inositol triphosphate (IP3) and Diaglycerol (DAG). IP3 interacts with several receptors in the Endoplasmatic Reticulum (ER), which results in Ca^{2+} release from its lumen. In addition, IP3 is metabolized by a protein kinase phosphorylating IP3 at position 3, forming inositoltetraphosphate (IP4), which acts as a second messenger implicated in controlling Ca^{2+} release through specific channels in the cell membrane. Ca^{2+} and DAG activate different cytoplasmic, as well as nuclear signalling cascades. It is also a well known fact that chemokines from the CC-family induce activation of Phospholipase A (PLA_2), and liberation of arachidonic acid in monocytes.

Phosphatinositol-3 kinase is an enzyme formed by a regulatory and a catalytic subunit which facilitate the entry of a phosphate group to position D3 of phosphatidyl inositol lipids. These lipids play a role in the signalling pathways implicated in cellular growth and the organization of the cytoskeleton. Upon binding of the chemokine to its receptor, the chemokine activates a heterodimer of PI3K, capable of phosphorylate PtdIns, PtdIns(4)P and PtdIns(4,5)P_2 which in

turn act as second messengers to proteins as PKC and AKT, in addition to the signalling pathways related to Ras [19].

The activation of neutrophils by chemoattractants results in activation of the GTPase Ras, which in turn activates the MAPK signalling cascade through binding of the Ser/Thr kinase Raf. Activation of MAPK through IL-8 binding to the receptors CXCR1 and CXCR2 transfected into Jurkat cells have also been described [20]. The MAPK signalling cascade has many functions, most of them related to gene expression controlling basic cellular mechanism, such as mitosis, cell proliferation, differentiation and survival or death.

1.2.2 Attachment of chemokines to the chemokine receptor

Most of the GPCRs belonging to Rhodopsine family contain two highly conserved cysteine residues, which form a disulfuric bridge between the first and second extracellular loop. The chemokine receptors contain two additional highly conserved cysteine residues, through which a second disulfuric bridge is formed, between the N-terminus and the third extracellular loop. These two bridges play important roles in the binding and correct positioning of the ligand and hence the capacity of the receptor to pass the signal on to the interior of the cell (Fig. 1.5).

The regions implicated in ligand binding have been identified through mutagenesis-based studies and by generating chimeric proteins. For some chemokine receptors, ex. CCR5, the N-terminus is critical for maintaining specificity to the different ligands. The globular domain of the chemokine interacts with the receptor through the second extracellular loop, thus reorienting the N-terminus so that it points to the transmembrane regions of the receptor [21]. The chemokine receptors undergo glycosylation and/or sulfation of tyrosine residues at the N-terminus [22]. These processes increase the affinity of the receptor to its ligands, and in the case of CXCR4 and CCR5, facilitate the entry of the Human Immunodeficiency Virus.

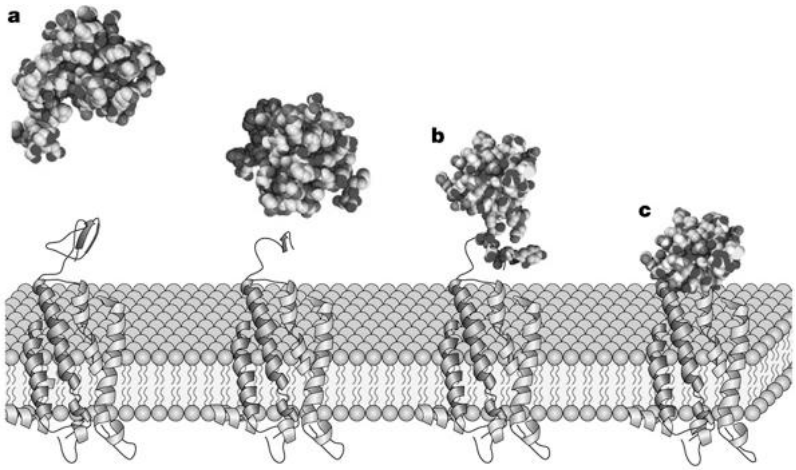

Figure 1.5: CCL5 attaching to its receptor CCR5. (a) The initial binding of the chemokine to its receptor is based on electrostatic interactions between the negative charge of the second extracellular loop of the receptor and the positive charge of the surface of the chemokine. (b) The first contact is made between the N-terminus of the ligand and the second extracellular loop of the receptor. (c) The ligand-receptor complex formed stabilizes the active form of CCR5 [23].

1.2.3 Oligomerization of chemokine receptors

The activity of GPCRs was originally related to the monomeric conformation of the receptors, but increasing evidence began to indicate that GPCRs can heterodimerize, or even oligomerize. The first evidence of these possible active conformations was published by Agnati et al. in 1980 [24], but it remained a controversial statement for a long time. Evidence showing that active forms of class A GPCRs always exist as either homo, heterodimers or oligomeric complexes has been published [25]. However, evidence claiming the monomeric form to be the functional unit, hence neglecting the existence of the dimers of this GPCR family also exists [26]. In the case of glutamate GPCRs, there is no doubt that the minimal functional conformation consists of dimers, and its mechanism for dimerization, as well as its signalling mechanism has been well studied. The transmembrane regions of this receptor play an important part in interaction with the G-protein. The α-helices of these regions are crucial for dimerization, in addition to several other domains of the receptor, as ex. the Venus Flytrap domain (VFT) at the N-terminus and the cysteine rich domains (CRD) located between VFT and the α-helices of the transmembrane regions. The glutamate GPCR dimers are believed to be covalent attached to each other, as several energy interactions, affinity and half life assays have shown them to be very stable [27]. Dimerization of the GPCRs can occur at different

regions, depending on the type of GPCR. Dimerization can occur at the N-terminus (glutamate receptors and ion channels), the C-terminus(γ-receptors) or at the transmembrane regions (the D2 dopamine receptors, and the β adrenergic receptors)[28]. For some receptors, dimerization is essential for localization in the cell membrane. This is for example the case of the $\beta_2$adrenergic receptors. Dimerization of these receptors occurs already in the ER [29], and they are transported to the cell membrane in this oligomeric form. It has been suggested that dimerization and activation of the glutamate receptors are interdependent, although recent studies indicate that only one of the two receptors forming the dimer are required for interaction with the G-protein. This supports the fact that the ratio of the dimer/G-protein complex is 1:1 [27]. This also corresponds with studies showing that regulation through interactions with arrestins only requires one of the two receptors of the dimer to bind to this protein [30].

As for the chemokine receptors, an increasing amount of evidence also proves that these GPCRs dimerize or oligomerize. Early experiments demonstrated that CXCR4, CCR5 and CCR2 form dimers [31-33]. At that point, and probably because of the instability of the complexes as a result of the treatment with several detergents, it was also concluded that the ligands promoted the formation of dimers. Later studies based on co-immunoprecipitation and energy transfer techniques like Bioluminescence Resonance Energy Transfer *(BRET)* and Fluorescence Resonance Energy Transfer *(FRET)* demonstrated that the homo- and heterodimers of CCR5 and CCR2 are present in the cell membrane in the absence of ligands [34, 35], and that the homodimerization of CCR5 occurs during synthesis in the ER [33]. In this receptor, the Ile52 and Val150 amino acid residues (in TMI and TMIV respectively) play an important role in the dimerization process, and mutation of either one of these amino acid residues disables the ability of the receptor to dimerize and thus results in loss of function [36]. The ability of several chemokine receptors as well as other GPCR mutants to dimerize with the non-mutants, and retain these in different intracellular compartments has also been described, as f. ex. the natural mutant CCR5Δ32S and CCR5 [37].

Differences in functionality between the different receptor conformations have been detected. For example, the signalling pathway of CCR2/CCR5 shows some differences compared to that of the homodimers alone. [38]. Another example is the heterodimer CXCR4/CXCR7, which intensifies the signalling promoted by CXCL12 during embryonic development [39].

Allosteric modulation of the chemokine receptor function after binding of an antagonist to one of the receptors has also been demonstrated. For example, binding of an antagonist to the *trans* complex CCR2/CXCR4, inhibits the binding of the ligand of the other [40].

Heterodimerization between CCR5 and CXCR4 was claimed not to exist in 2002 [33]. Later, it was demonstrated that heterodimers of CCR5 and CXCR4 are formed in activated T-cells in the immunological synapses, where they act together as an oligomeric complex promoting a specific signalling pathway [41]. In 2008, heterodimers of CXCR4 and CCR5 were described outside the immunological synapse in FRET studies [42] and subsequently in BRET studies in 2009 [43]. It has also been showed that the respective ligands of CCR5 and CXCR4 modulate the dimer conformations in opposite manners, as the ligand of CXCR4 decrease dimer formation while the ligand of CCR5 promotes heterodimerization between CCR5 and CXCR4 [42].

There are still many cases of homo- and heterodimerization between chemokine receptors left to discover, as well as between other GPCRs. Recent evidence even indicates that both receptor expression and ligand binding modulate the chemokine receptor conformations [44]. Oligomerization of the chemokine receptors is thus today a well accepted phenomenon. Current debates revolve mainly around the functional relevance of the different conformations, if or to which extent they are dynamic and, if so, what controls their dynamics.

1.2.4 CXCR4, CCR5 and their ligands in physiological and pathological processes

The chemokine receptors and their ligands are implicated in a vast multitude of physiological, as well as pathological processes. Although a specific chemokine can bind to various receptors and one specific receptor can interact with various chemokines, each binding results in a specific cellular signal, depending on the cell at which the binding takes place, its localization in the body and the physiological status of the cell at the moment of the signalling. In the following sections, the most important pathological and physiological functions of CCR5, CXCR4 and their respective chemokines (CCL5 and CXCL12) will be shortly discussed.

1.2.4.1 Embryonic development

CXCL12 and its receptor CXCR4 (as well as CXCR7) play a very important role in embryonic development. Deletion of CXCR4 or CXCL12 in mice gives rise to a lethal phenotype, characterized by several cardiac defects (dysplasia of the septic ventricle), hematopoietic defects (deficiency of lymphopoiesis of B-cells and myelopoiesis of the bone marrow) and abnormal development of the cerebellum [45].

1.2.4.2 Immune system

Homeostasis of the immune system depends completely upon mobility of the immunological cells. The hematopoietic precursors complete their differentiation in an adult individual through a process in which CXCR4/CXCL12 interaction is essential [46]. CXCR4 also contributes significantly to the lymphatic recirculation ("homing") of B-cells to the lymph nodes.

1.2.4.3 Tumours

Even though angiogenesis and metastasis are two similar processes involving cell mobility, there are mechanisms by which tumours metastase independently of angiogenesis. CXCR4 and CXCL12 seem to be of major importance in the metastasis of breast cancer tumours to the lungs (generally one of the first organs to which metastasis occurs)[47]. Other cancer types metastase through other chemokine receptors.

1.2.4.4 Autoimmune diseases

CXCR4, CCR5 and their ligands also play a role in autoimmune illnesses [48] and regulation of the neuroendocrine system [47, 49]. It has for example been demonstrated that CXCL12

and CCL5 are involved in Rheumatoid Arthritis [50], multiple sclerosis [49, 51]and in Diabetes type I [52].

1.2.5 The Role of CXCR4 and CCR5 in HIV Infection

CXCR4 and CCR5 are perhaps best known as the co-receptors of the Human Immunodeficiency Virus type 1 (HIV-1), the causative agent of Acquired Immunodeficiency Syndrome (AIDS). HIV infection of white blood cells (lymphocytes and monocytes) occurs through binding of a viral envelope glycoprotein called gp120 to CD4 and CXCR4 and/or CCR5 (Fig 1.6) [53], depending of the viral strain in question. The X4 (T-tropic) strain infects lymphocytes (T cells), while the R5 (M-tropic) strain infects monocytes. Dual-tropic strains infecting both cell types exist, using both co-receptors [54] Binding of the envelope glycoprotein to CD4 and the chemokine receptor(s), leads to membrane fusion, and the viral genome enters the host cell, integrating viral DNA, after reverse transcription of RNA, in the host cell DNA. The host cell starts producing viral proteins, including new envelope glycoproteins which are transported to the host cell surface where they can assemble with other viral proteins to form new virion particles. The break-through discovery regarding the role of CCR5 and CXCR4 in HIV infection turned these chemokine receptors into very promising HIV therapy targets, and some of the currently available HIV drugs act on these receptors. Individuals with natural mutations of the CCR5 receptor exist (CCR5Δ32), having a significantly reduced risk of infection or a delay in the development towards AIDS [31]. CCR5Δ32 is not transported to the cell membrane and is therefore rapidly degraded. It is, however, capable of dimerizing with CCR5, retaining this receptor in different intracellular compartments and decreasing its expression in the cell membrane [37]. Some scientists proposed a possible negative dominance of the mutant as an explanation for the delay in the development of HIV towards AIDS, but this was later rejected, as it was demonstrated that the decrease in the expression of CCR5 in the cell membrane was due to a decrease in gene dosage [55].

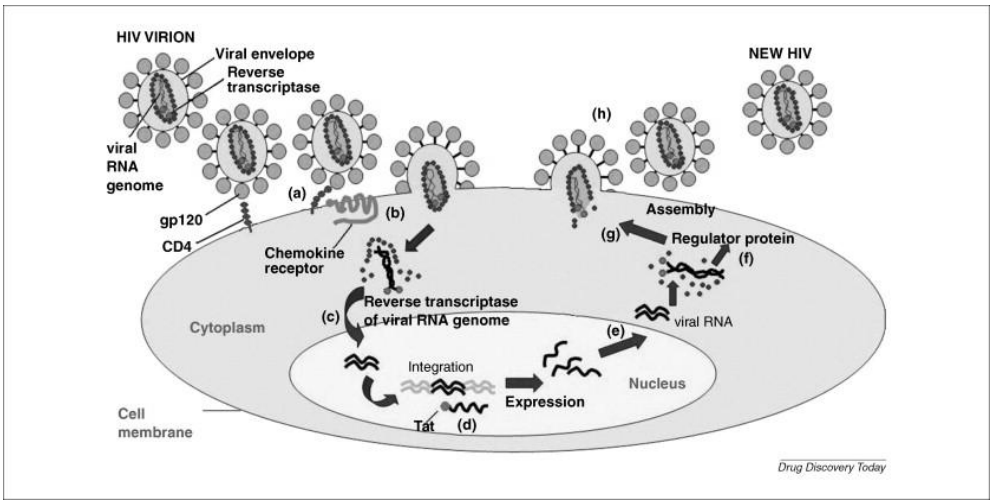

Figure 1.6: The reproductive cycle of HIV. (a) Binding. The HIV virion binds to the CD4 receptor, and subsequently to the co-receptor(s). (b) Fusion. HIV fuses with the cell membrane. Virion core is released into the host cell. (c) Reverse transcription. The single stranded viral RNA is converted to double stranded viral DNA. (d) Integration. The double stranded viral DNA is integrated into host cell DNA. (e) Transcription. Host cell RNA polymerase copies the HIV genomic material and generates messenger (m) RNA. Long chains of viral proteins are produced from the mRNA. (f) Regulator proteins. Increase HIV gene expression dramatically. (g) Assembly. The long chain of viral proteins is hydrolyzed and cut into small functional proteins by the HIV enzyme protease. New virions are formed with the small functional proteins and new RNA. (h) Budding. The new virion uses a cellular envelope as cover and exit the host cell through budding. Taken from www.drugdiscoverytoday.com

The external envelope glycoprotein (gp120) of HIV binds to the CD4 receptor on the cell, and this binding promotes a conformational change in the gp120 envelope, resulting in the exposure of a domain known as the CD4 induced (CD4i) domain. This domain, in conjunction with the third hypervariable region (V3 loop) of the HIV is crucial for recognition and binding to the co-receptors [56]. The details of this mechanism are currently not clear, but it is likely to be complex, as both the CD4i domain and the V3 loop are implicated. Studies have also demonstrated that the V3 loop is a major determinant of HIV-1 tropism. The V3 loop is a surface-accessible loop formed by a disulfide bridge between two invariant cysteins at positions 296 and 330 of gp120 [57]. Two functionally distinct regions of gp120 for binding to CCR5 have recently been discovered, designated as the stem and the crown. Both have been shown to be necessary for binding, but the V3 crown alone determines the receptor specificity of the virus [58]. It has also been demonstrated that the R5 virus dominates in early infection, but that the virus switches to X4 in about 50% as the disease progresses. This switch is associated with a worsening of prognosis, and is hence of importance in a direct

clinical context. There are several hypotheses explaining this receptor preference switch, but no mechanism or reason for the switch has been determined yet [59]. Medicinal treatment of HIV-1 infection normally involves a mixture of drugs with different mechanisms of action, as for example protease antagonists, reverse transcriptase blockers and fusion inhibitors. Several CCR5 and CXCR4 antagonists have shown themselves able to decrease infection *in vitro*, but this may not be related to *in vivo* conditions. In Norway, Maraviroc® is the only drug existing with a chemokine receptor antagonist mechanism. This drug binds to CCR5 at its ligand binding site and thereby blocks binding to the viral gp120 envelope. Maraviroc® has no effect on T-tropic HIV-1 at all *in vivo*. The necessity of finding new strategies based on the chemokine receptors to block or decrease infection is therefore highly present, and revealing the dynamics of the conformations of the receptors implicated in HIV infection may contribute importantly to this.

1.3 Techniques

1.3.1 Flow Cytometry

Flow Cytometry is a powerful technique used to identify the properties of individual cells within heterogeneous populations, suspended in fluid. Cells are labelled with a fluorescent antibody, and passed one by one through a laser beam. The light emitted as the cells pass through the laser beam is collected by the cytometer and processed by a suitable data system.

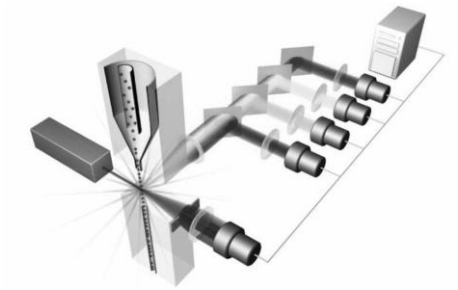

*Figure 1.7: The different elements of a flow Cytometer. (*flow.csc.mrc.ac.uk/?page_id=302)

A cytometer consists of three main parts:

The fluidic system

The main point of the fluid system is to disperse the cells randomly in fluid, and transport them one by one to the interrogation point. The flow cell is a major part of the fluidic system. This consists of a narrowing core channel, through which the cell sample is injected under pressure. Surrounding this core channel is an outer and bigger channel filled up with sheath fluid. Due to the physics of the flow cell, the outer channel always has a lower pressure than the core channel, but the fluid flows faster than the injected cell sample. This difference in pressure and velocity between the two channels creates a huge drag on the injected cell sample, which allocates the cells in a row, forcing them to pass one by one through the laser beam. This effect is called hydrodynamically focusing [60].

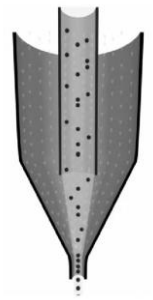

*Figure 1.8: The flow cell of a cytometer. (*flow.csc.mrc.ac.uk/?page_id=302)

The laser

The laser is the light source and it is responsible for the emission of light from the cells. The light scattered from the cell is gathered and directed to detectors which collects the light at specific wavelengths.

The electronics/ data system

Light emitted is transformed into quantitative results by suitable data systems. These systems may vary depending on the laboratory and the purpose of the experiment.

Several flow Cytometry-based techniques have been used in this project:

1.3.1.1 Calcium Assays

Calcium assays were performed in order to assure the physiological function of the cells in spite of a fluorescent protein attached to the receptor. As activation of the chemokine receptor release calcium flux from the ER in the cell, the function of the receptor can be determined by measuring the calcium flux upon activating the receptor with its respective chemokine. Fluo-3 AM was used as a Calcium indicator, having its excitation wavelength in the green fluorescent spectrum. Fluo-3 acts as a calcium chelator in the cells, enabling visualization of the calcium flux upon receptor activation.

1.3.1.2 Staining

Staining has in this project been performed in order to determine the percentage of receptors expressed at the cell surface. Low expression could be a consequence of the transfection process, old, overgrown or in other ways damaged cells, internalization of the receptor or poor

DNA quality. The cells were incubated with a specific antibody to the receptor of interest, and this antibody is then attached to a secondary antibody labelled with a fluorescent colour enabling identification of the receptor by flow Cytometry.

1.3.2 Resonance Energy Transfer (RET)

The technique of RET is based on the quantitative theory of energy transfer through resonance, developed by Förster (1946-1949). It is used to study the interaction between two proteins, with one acting as a donor (D), and the other as an acceptor (A). In an electronic exited state, the donor will transfer energy to the receiver through dipole-dipole interactions, only if the donor and the acceptor are located close enough. As the acceptor absorbs all the energy from the donor there is no loss of energy, hence no emission of photons and the whole process is therefore non-radioactive.

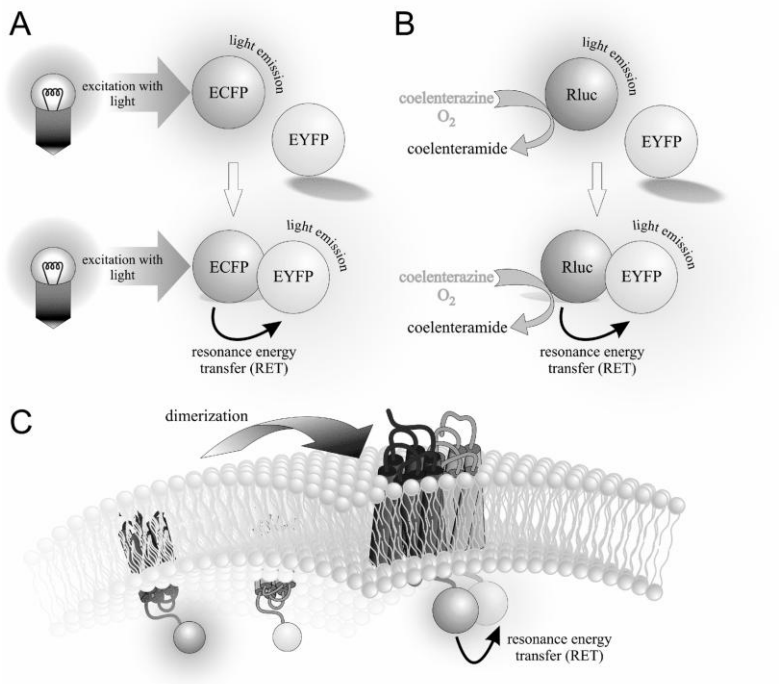

Figure 1.9: Mechanism of A) Fluorescence Resonance Energy Transfer (FRET) and B) Bioluminescence Resonance Energy Transfer (BRET). C) RET shown in the context of dimers in the cell membrane [61].

Two techniques have been developed to take advantage of this principle in *in vivo* studies; Fluorescence Resonance Energy Transfer (FRET) and Bioluminescence Resonance Energy Transfer (BRET). These are very similar techniques, only differenced by the type of luminescence markers. FRET has been used in this project.

1.3.2.1 Basic Principles of FRET

FRET is based on the techniques explained in Section 2.2.1, with at least one of the two proteins studied being fluorescent, although laboratories prefer both of the proteins in FRET experiments to be fluorescent. The characteristic fluorometric spectra of the different fluorescent proteins allow the energy transfer between these to be modulated and measured.

A) *B)*

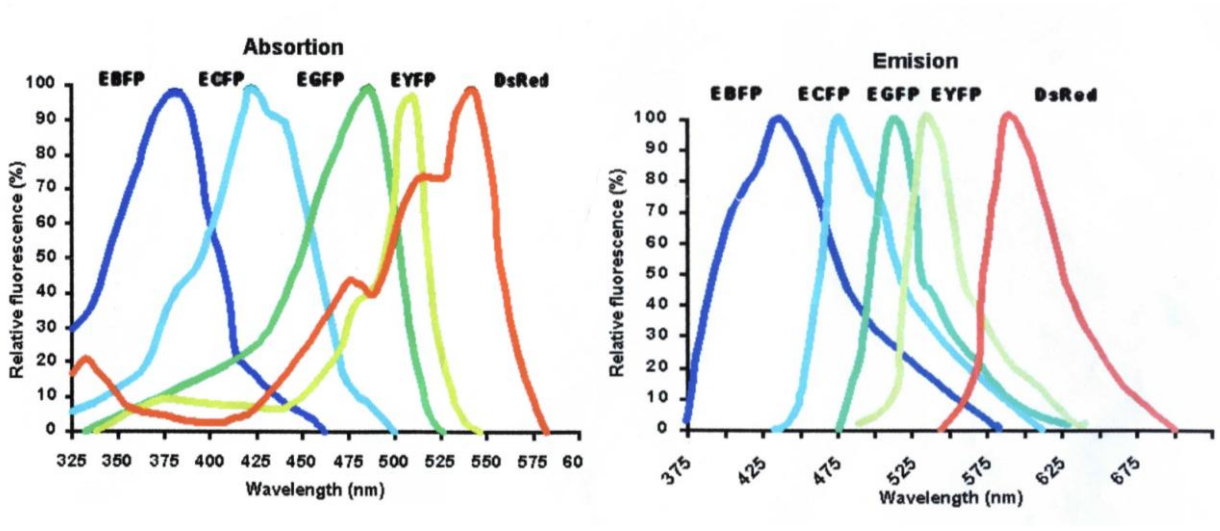

Figure 2.4: A) Absorption and B) Emission spectra of the different fluorochromes. (Dep. of Oncology & Immunology, CNB, Madrid, Spain).

It is of major importance that the fluorescent donors and acceptors fulfil certain requirements;

1- The emission spectrum of the donor should overlap the absorbance spectrum of the acceptor.

2- Donor and Acceptor should be sufficiently aligned for the dipole-dipole energy transmission to be possible. The orientation of the proteins is also of importance and a major factor to consider when analyzing the energy transfer between the two.

3- The distance between the two proteins should be approximately 10 nanometres for the energy transfer to be possible. Each pair of fluorescent proteins has its specific distance.

FRET PAIR	Exmax DONOR (nm)	Em-max ACCEPTOR (nm)
BFP2-mGFP	383	507
CFP-YFP	440	527
Cerulean-Venus	440	528
GFP-mCherry	489	510
Venus-mCherry	528	610
Venus-tdTomato	528	581
Venus-mPlum	528	649
Cy3-Cy5	554	670
GFP-Cy3	489	566
GFP-YFP	489	527

Table 1.2: FRET pairs with their respective donor and acceptor excitation and emission wavelengths. Courtesy of Laura Martinez-Muñoz, CNB, Madrid.

According to Förster's theory, the efficiency (E_t) of the energy transfer is inversely proportional to the sixth potency of the distance that separates the two proteins. This gives

$E_t = R_0^6 / R^6 + R_0^6$

R = the distance separating the two fluorescent proteins

R_0 = the distance separating the donor and the acceptor where 50% of the exited energy is transferred from the donor to the acceptor, and the other 50% is either lost to radiation or not. The efficiency of the energy transfer is in other words highly dependent on the distance between the two fluorescent proteins.

Positive FRET signals hence indicate protein interaction. It is, however, important to be aware of the fact that negative FRET signals are not necessarily suggesting lack of dimerization.

There are several methods of measuring the efficiency of FRET, once the donor has been excited. I will discuss two of these methods, which have been used in this project.

1.3.2.1.1 Acceptor Sensibilization (Saturation Curves)

This method is perhaps the simplest in order to detect FRET efficiency. FRET can be measured using a confocal microscopy, taking only one cell into consideration at a time, or it may be measured through a fluorescence lector with specific detectors, taking whole cell populations into account (Section 3.7). The fluorochrome of the donor protein is exited at its specific wave length and the emission of light is obtained through two detection filters which detect wavelengths equivalent to that of the donor and the acceptor. The saturation curves of FRET are obtained by maintaining the quantity of CFP (fused to the donor receptor) and varying the quantity of YFP (fused to the acceptor receptor). By doing this, different ratios of YFP/CFP are obtained, and the efficiency of FRET can be calculated for each ratio. Cells expressing only YFP (pEYFP-N1) or CFP (pECFP-N1) serve as an internal control, while cells co-expressing both CFP and YFP without any receptor, serve as a positive control. FRET is measured by the use of an excitation filter of 400 nm (ranging between 393 nm – 403 nm) and two emission filters of 510 nm ± 8 and 530 ± 8 nm for CFP and YFP, respectively. Emission is collected in both channels, and the same conditions are maintained during the whole measurement process, so that the relative contribution constants of the fluorophores in the detection channels are kept unchanged. This would be a perfect way to measure FRET, but one problem exists; exciting the donor protein will always result in a certain amount of excitation and emission from the fluorochrome of the acceptor protein as well, although this has a higher excitation wave length. Therefore, some of the FRET shown when exiting the donor protein may not be due to FRET, but to an actual excitation of the acceptor protein. This effect is called “crosslinking”, and as a consequence, control measurements are needed in order to find the true FRET efficiency value. FRET must be measured in cells expressing only the donor protein fused to its fluorescent protein and cells expressing only the acceptor protein fused to its fluorescent protein. The FRET efficiency obtained in these cells enables the determination of the amount of crosslinking between the excitation and the emission channel, and it is used to normalize the FRET values of the cells co-expressing the donor and

the acceptor fused to CFP and YFP, respectively. Zimmerman et al. have developed several mathematical equations in order to calculate the fluorescence emitted individually by the donor and the acceptor independently, taking all the above mentioned parameters into consideration (Spectral Un-Mixing) [62]. These equations have been used in this project:

$Q = Ch_{510\ nm} / Ch_{530}$

$R = (YFP_{530\ nm}\ Q - YFP_{510}) / (CFP_{510\ nm} - CFP_{530\ nm}\ Q)$

Where $Ch_{510\ nm}$ and Ch_{530} represent the detected signals in the channels of 510 nm and 530 nm, respectively.

The normalized values of the fluorescent proteins FluoCFP and FluoYFP in the channels of 510 nm and 530 nm, calculated with the control samples of CFP and YFP alone, are represented as $YFP_{530nm510nm}$ and $CFP_{510nm530nm}$.

Fluorescence is then calculated for each of the proteins:

FluoCFP = S/ (1+(1/R))

Fluo YFP = S / (1+R)

Where $S = Ch_{510nm} + Ch_{530nm}$

Hence, FRET efficiency is:

$FRET_{eff}$ = Fluo YFP / S

The calculated FRET efficiency values are put into a graphic system where the x-axis represents the ratio YFP/CFP, and the y-axis represents the FRET efficiency measured. A theoretic parameter also used is that of $FRET_{50}$, reflecting the ratio at which 50% of the receptors undergo FRET. This value can be regarded as the apparent affinity of the two receptors.

Due to the mathematical equations for calculating the FRET efficiency, only the FRET values of saturation curves with at least one receptor in common can be compared to each other. Thus, the FRET values of the homodimers of two receptors cannot be compared, but the FRET values of their respective heterodimer can be compared to those of their homodimers.

1.3.2.1.2 Acceptor Photobleaching

This method requires the use of a confocal microscope. It is based on the fact that the intensity of the fluorescence of the donor is decreased in the presence of FRET, because a major part of the exited energy is transferred to the acceptor. When the acceptor protein is bleached by the use of specific lasers, the extinction effect of the acceptor towards the donor is eliminated, and as a consequence, the fluorescent intensity emitted by the donor increases significantly. Care must be taken as the acceptor protein is bleached, so that the donor protein is not degraded. Four separate images are taken of the receptors coupled to CFP and YFP in a selected cell region, before and after bleaching (CFPpre, CFPpost, YFPpre and YFPpost). FRET efficiency can then be considered as;

$$E = 1-(I_{da}/I_d)$$

Where:

1- I_{da} = the intensity of the donor's fluorescence after bleaching the acceptor

2- I_d = the intensity of the donor's fluorescence before bleaching the acceptor

One of the major advantages of this method is that it enables us to study the interaction between two proteins of a single cell at the time, focusing on specific parts of the cell, for example the cell membrane, as has been done in this project. However, the photobleaching method has some disadvantages. Dynamic studies are impossible, as the cells are fixed. In addition to this, Photobleaching is a destructive technique, as the acceptor protein is destroyed in the process. Furthermore, it allows us to measure the FRET of each cell only once. The results obtained are also only based on one cell, and the interaction between the two proteins in a specific region of this cell. Several images should therefore be taken during the experiment (approximately 50-100 cells), in order to obtain FRET efficiency which is representative of the population. However, one should keep in mind that images of 100 cells are still a very minor pool of any cell population. When using the photobleaching method, certain things should be taken into consideration;

1- Functionality and maintained levels of the proteins in question should be assured, as they are fused to a fluorescent protein. Functional assays should therefore be completed before initiating further experiments.

2- Because the cells are cotransfected, it is essential that the levels of both the donor and acceptor proteins are determined. The intensity of the emission of the fluorescence of both should be similar; they should thus exist in a ratio of approximately 1:1.

A specific plugin measures pixel by pixel of the 4 separate images taken (CFPpre, CFPpost, YFPpre and YFPpost), with a correct donor/acceptor ratio, bearing in mind the pixel number of CFP and YFP before and after bleaching the acceptor protein, and the percentage of bleaching of the acceptor protein. The plugin also subtracts the intensity background of CFP from every image and analyzed region (pre and post). FRET efficiency is hence calculated according to the following formula:

$$E_{FRET} = ((ICFP_{post} - ICFP_{pre}) / ICFP_{post}) \times 100$$

Where:

$ICFP_{pre}$ = The emitted florescence collected of CFP before bleaching

$IYFP_{pre}$ = The emitted florescence collected of YFP before bleaching

$ICFP_{post}$ = The emitted florescence collected of CFP after bleaching.

As negative controls, the fluorescence intensity (pixels) of CFP is measured in cells only transfected with CCR5 CFP before and after bleaching. The percentage of FRET efficiency obtained in these controls is subtracted from all the other evaluated images of cells containing both donor and acceptor proteins. FRET efficiency is finally calculated by the mean value of three independent experiments, each of which containing at least 50 images. Although fluorescence oversaturated regions are intentionally avoided as the experiment is carried out, the fluorescence of CFP and YFP in oversaturated regions are determined in the images before bleaching, using the program ImageJ, so that only regions with a ratio YFP/CFP of 1-1.5 are included in the analysis.

1.3.3 In Vitro Determination of T-tropic HIV-1 Infection by Cell-Cell Fusion Assay

HIV-1 infects cells by interacting with the receptors CD4 and CXCR4 or CCR5. Infection capacity can be evaluated by monitoring cell-cell fusions between cells containing the envelope glycoprotein gp120 (effector cells) and cells containing the necessary receptors for infection (target cells), using Firefly and Renilla Luciferases as reporters. The target cells are co-transfected with Firefly and Renilla Luciferases under the control of a T7 promoter. Firefly and Renilla Luciferases catalyze reactions resulting in light emission as beetle luciferin and coelenterazin, their respective substrates, are added.

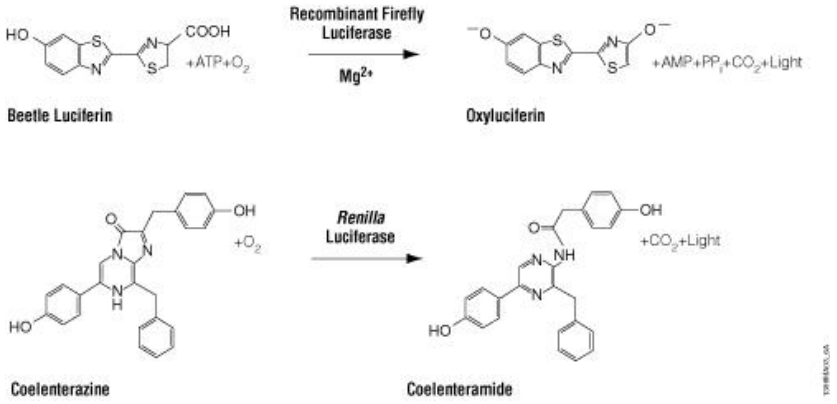

Figure 2.5: The catalytic reactions of Firefly Luciferase (above) and Renilla Luciferase (under). Taken from www.promega.com

As Firefly and Renilla Luciferases are both intracellular proteins, cell lysis prior to assessing light intensity is necessary. The commercial kit (Dual-Glo® Luciferase Assay System (Promega) used in these experiments, allows for independent measurements of both Firefly and Renilla Luciferase bioluminescence, as the Renilla Luciferase substrate solution contains a reagent quenching the Firefly Luciferase reaction, decreasing it approximately 10 000 fold. As the T7 promoter is activated by the T7 DNA polymerase upon fusion of the effector cells and the target cells, light intensities produced by Firefly Luciferase can be considered as a reflection of the infection occurred. The Firefly Luciferase intensity in non-infected cells can be considered as background luminescence, as these cells have not fused with the effector cells, and hence do not contain the T7 promoter. The light intensity produced by the reaction catalyzed by Renilla Luciferase does not depend on the cells being infected or not, it only

depends on the amount of DNA transfected. Thus, the light obtained from the Renilla Luciferase catalyzed reaction is used for calculating Firefly /Renilla Luciferase ratios from the different cell samples, normalizing each sample in order to avoid falsification of the results by background luminescence. The relative ratio of each point is finally calculated by dividing the normalized experimental ratios of the infected cells, by the normalized negative control ratios of the corresponding non-infected cells. The relative ratios of the infected cells can be compared, and a decrease in value reflects less infection.

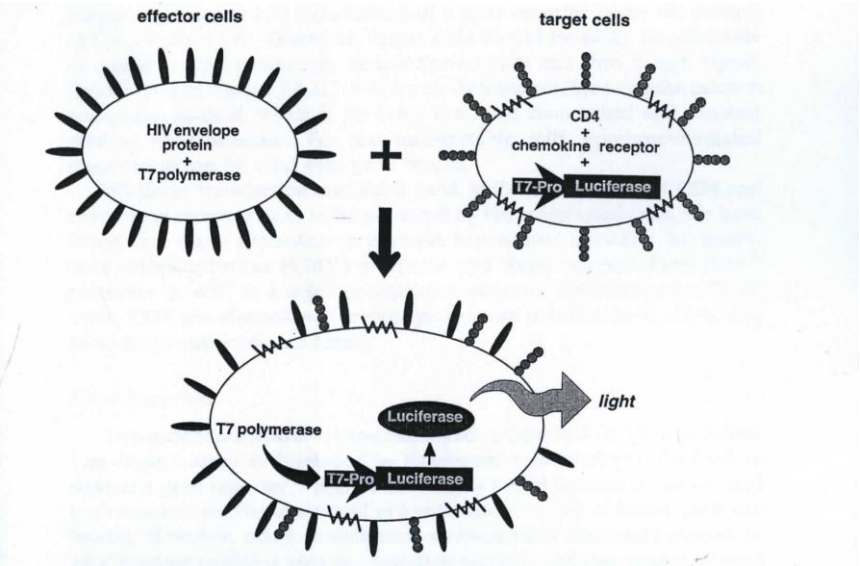

Figure 2.6: Cell-cell fusion of effectors and target cells [63].

1.3.4 Internalization Assays

Upon stimulation with their respective ligands, the chemokine receptors internalize into the cell, and disappear from the cell membrane. This is a good way of measuring the effect of the presence of a certain chemokine receptor, as the whole receptor is removed from the cell membrane. Internalization can be visualized by for example Flow Cytometry staining, using antibodies against the specific receptor. The minimum intensity of the peak is of importance in these assays, as this value represents the mean intensity of the fluorescence of the receptors. As the receptor internalizes, the minimum intensity value decreases.

1.3.5 Protein Quantification by Bradford's Method

Bradford (Bio-Rad Protein Assay) is a protein quantification assay, in which a differential colour change of an acidic dye occurs upon reaction with varying amounts of proteins in an acidic solution. Measurement is done at 595 nm, and protein concentration can be calculated by extrapolating a standard curve, where the x- axis represents the concentration (mg/ml) and the y- axis represents the light absorbance.

MATERIALS & METHODS

Science is not belief, but the will to find out.
-Anonymous

2.1 Vectors and Constructions

The human receptors CXCR4 and CCR5, kindly donated by Dr. B. Moser (Cardiff University), were amplified by PCR from pcDNA3- CXCR4 or pcDNA3-CCR5 constructs using specific oligonucleotides, and cloned into pECFP-N1 and pEYFP-N1 (Clontech). Routinely, all generated plasmids were sequenced to assure correct ligation of DNA into the vectors. The oligonucleotides (primers) used were:

CXCR4_CFP/CXCR4_YFP:

Forward: 5´HindIII(5´CTCAAGCTTCGAATTCTGCAGATGTCCATTCCTTTGCCTTTG CCTCTTTTG3´)

Reverse: 3´AgeI(5´GACCGGTGGATCCCGTAAGCTGGAGTGAAAACTTGAAG3´)

CCR5_CFP/CCR5_YFP:

Forward: 5´HindIII(5´TAA AGC TTA TGG ATT ATC AAG TGT CAA GTC C 3´)

Reverse: 3´AgeI (5´GAC CGG TAA TAA CAA GCC CAC AGA TAT TTC 3´)

2.2 Cell lines

The cell lines HEK293 and 293T Italy (human kidney embryonic cells) were obtained from the American Type Culture Collection. The cells were cultivated in DMEM (Biowhittaker, USA) supplemented by 10% (v/v) Foetal Bovine Serum (GIBCO), 2 mM L-Glutamine and 1 mM sodium pyruvate. Cells were diluted every 48 hours, and cultured at 37°C and 5% CO_2.

2.3 Chemokines and Antibodies

The chemokines CCL5 (Rantes) and CXCL12 (SDF-1α) were obtained from Peprotech (London, England). The antibodies used were anti human CCR5 (Biolegend, California,

USA.), anti human CXCR4 (R&D Systems, Minneapolis, USA) and anti human CD4-PE (Beckman Coulter, England.)

2.4 Transient Transfection Assays

All the experiments included transiently transfected cells by JetPEI (Polyplus Transfection), except the FRET saturation curves which required transfection by polyethylenimine PEI (SIGMA-Aldrich). 293T Italy cells were plated in suitable plates and transfected with the vector(s) of interest 24 hours later, according to the manufacturer's protocol. Experiments were carried out after 48 hours incubation at 37°C and 5% CO_2. Transfection of Firefly and Renilla Luciferases only required 24 hours of incubation at 37°C and 5% CO_2.

Transfection by jet PEI included;

Mixture 1: 50 µl of 150 mM NaCl per 3 x 10^{10} cells + the correct amount of DNA of the receptor of interest.

Mixture 2: 50 µl of 150 mM NaCl per 3 x 10^{10} cells + 2 x the amount of DNA of JetPEI.

Both mixtures were vortexed during approximately 10 seconds. Mixture 2 was added to mixture 1 and the mixture was vortexed for another 10 seconds. The mixture was then left to incubate 30 minutes at room temperature, after which it was added droplet by droplet to the cell plate. The whole process was done in lamina flow hoods.

Transfection by PEI included;

Mixture 1: 25 µl of 150 mM NaCl per µg DNA (minimum 200 µl 150 mM NaCl). Vortexed for 10 seconds.

Mixture 2: 150 mM NaCl and PEI (5.47 mM nitrogen residues) in a ratio of 5:1.

Mixture 2 was added to mixture 1 in a ratio of 1:1 and vortexed for 10 seconds. The mixture was then left to incubate at room temperature for 15-30 minutes, after which non-supplemented DMEM was added to the mixture, in order to add a volume of 1.5 ml/$8x10^5$ cells to each well of cells. After 4 hours of incubation at 37 ℃ the cell medium was replaced by 2 ml 10% (v/v) supplemented DMEM per $8x10^5$ cells. The experiment was carried out 48 hours of incubation at 37℃.

2.5 Calcium Flux Assays

293T Italy cells were transfected with the fluorescent receptor of interest using JetPEI according to the protocol of the fabricant. 48 hours later, the transfection of the cells was assured by microscopy. The cells were then lifted with 0.2% (v/v) Ethylene Diamine Tetra Acetic acid (EDTA) and $5x10^5$ cells per sample were resuspended in 250 µl supplemented 10% (v/v) DMEM per sample. Fluo-3 was added (16 µl/ 10^6 cells) to the cells. Protected from light, the cells were left to incubate at 37℃ for 30 minutes under constant movement. After incubation, the cells were washed with 10% (v/v) supplemented DMEM and centrifuged at 1200 rpm for 5 minutes after which they were resuspended in 1 ml 10% (v/v) supplemented DMEM per $0.5x10^{10}$ cells. 2 mM $CaCl_2$/ $0.5x10^{10}$cells was added and the cells were divided into the correct amount of duplicated samples and added to Cytometry tubes. Cells were left at 37℃ for approximately 5 minutes, before they were analyzed by flow Cytometry (Coulter Epics XL-MCL)

2.6 Receptor level determination by Flow Cytometry staining

Cells were transiently transfected by JetPEI with the receptors of interest, according to the manufacturer's protocol. 48 hours later, $2.5x10^5$ cells per well were resuspended in 100 µl PBS staining (PBS + 1% (v/v) Foetal Bovine Serum + 0.5% (w/v) Bovine Serum Albumin) per well and placed in transparent plates of 96 wells with v-shaped bottoms. Following centrifuging at 1200 rpm for 5 minutes, the primary antibody was added at its correct concentration and left to incubate for 30 minutes. Cells were then washed with PBS staining

and centrifuged at 1200 rpm for 5 minutes, before the secondary antibody containing a specific fluorochrome was added at its correct concentration and left to incubate for 30 minutes. Cells were then washed with PBS staining, centrifuged at 1200 rpm for 5 minutes and resuspended in 100 µl of PBS. The cells were added to approximately 200 µl isotone in special Cytometry tubes, and passed through the flow cytometer (Coulter Epics XL-MCL)

2.7 Saturation Curves

Plating

$4x10^5$ cells per well were plated in plates of 6 wells (p6w) in a volume of 2 ml 10% (v/v) supplemented DMEM per well, in the necessary wells to duplicate the predetermined amount of YFP/CFP ratio points, and the necessary controls (Section 1.3.2.1.1). Cells were then left to incubate at 37ºC and 5% CO_2 for 24 hours.

Transfection

24 hours after plating, the cells were transfected with the relevant receptors fused to fluorescent proteins, in order to obtain both YFP/CFP ratios of the receptors, and the different control samples (Section 1.3.2.1.1) by PEI, each well separately, in duplicate. Cells were then left to incubate in 10% (v/v) supplemented DMEM at 37ºC and 5% CO_2 for 48 hours, after which the transfection of the cells was assured in the microscope, checking that YFP amounts increased in correlation to the amount transfected in every point, and that CFP was maintained in all points.

Measurement

The cells in each well were then lifted and washed with 1 ml of Hanks Balanced Salt Solution (HBSS) supplemented with 0.1% (w/v) glucose at 37 ºC. Cells were centrifuged at 1200 rpm for 5 minutes. The cells in each well were then resuspended in 240 µl of the same supplemented HBSS. As each well needed to contain the same amount of protein, the protein amount was quantified by Bradford's method (2.9), and the protein amount was adjusted to 0.2 µg/µl per point. 100 µl of each point were finally added to black plates of 96 wells, every

point distributed in duplicates, and fluorescence was analyzed by the fluorimetre Wallac Envision 2104 Multilabel Reader (Section 1.3.2.1.1).

2.8 Acceptor Photobleaching

Plating

10x10 mm crystals were deposited in plates of 24 wells (p24w), draped with poly-L-lysine (20 µg/ml, diluted in PBS) and left to incubate for 1 hour at 37°C. $5x10^4$ cells per well were then plated over the crystals in a volume of 500 µl of 10% (v/v) supplemented DMEM and left to incubate for 24 hours at 37°C and 5% CO_2.

Transfection

The cells were transfected with the corresponding receptors fused to fluorescent proteins by JetPEI, according to the manufacturer's protocol, and left to incubate in 10% (v/v) supplemented DMEM at 37°C and 5% CO_2 for 48 hours. After incubation, the transfection of the cells was assured by microscopy.

Measurement

The cells in each well were treated with 4% (v/v) Formaldehyde during 2-3 minutes, in order for the cell conformations on the crystals to freeze (fixate). Afterwards, the cells were washed several times with PBS. Using a drop of glue solution (80% (v/v) glycerol and 20% (v/v) PBS at pH 7), the crystals were glued onto a microscope slide, preventing bubble formation. The edges were fixed with blank nail polish and left to dry, before analyses by confocal microscopy. The microscope slides were stored in the dark, due to the fluorescence, and at 4°C due to the instability of the glue solution. The samples were analyzed by the confocal microscope Olympus Flowview 1X81. Different lasers were used in order to excite the donor (D) and the acceptor (A) protein. The donor protein (D), in this case CCR5 CFP, was excited using a diode laser of 405 nm wavelength (12% potency: 25 mW), while the acceptor protein (A), being CXCR4 YFP, was excited using an argon laser of 515 nm wavelength (10% potency: 45 mW). A dual dicroic mirror of 405-440 / 515 nm was used in both cases. The emitted florescence passed through a dicroic mirror of SDM 510 nm and was collected by a

detector in the range between 460-500 nm for CFP ($ICFP_{pre}$). The fluorescence emitted by YFP was collected by filtrating light in a range between 530-570 nm ($IYFP_{pre}$). The YFP protein was bleached by increasing the argon laser of 515 nm to maximum potency during approximately 5-10 seconds. Once 60-90% elimination of the YFP protein was achieved, fluorescence intensities of CFP and YFP were measured again, using the same parameters as before (ICFP post, IYFP post). FRET efficiency was finally determined using the program IMAGE J 1.37r (Wayne Rasband) (Section 1.3.2.1.2).

2.9 Protein Quantification by Bradford's method

200 µl of 20% (v/v) Bradford solution diluted in HBSS was added to the necessary wells of a plain-bottomed transparent plate of 96 wells. 20 µl of each cell sample was added to a well containing the Bradford solution, in addition to a standard curve. Light absorbance was measured in the fluorimetre Tecan Infinite M200.

2.10 Cell-Cell Fusion Assay

Cells from the cell line HEK 293 were chosen as target cells for this assay, because they express CXCR4 endogenously. HEK 293T cells were used as a negative control, as they do not contain the CD4 receptor, and stable HEK 293 CD4 cells were used as a positive control, as they contain both co-receptors necessary for T-tropic gp120 binding. Two cell lines containing different amounts of CCR5 were used to measure T-tropic viral infection in the pilot cell-cell fusion assay. HEK 293 CD4 cells transiently transfected with increasing amounts of CCR5 were used in further cell-cell fusion assays.

Plating

Target cells

$1.5x10^5$ cells per well of each cell type (negative control, positive control and cells containing CCR5) were plated in duplicate, in a volume of 1 ml 10% (v/v) supplemented DMEM in plates of 24 wells (p24w), and left to incubate at 37°C and 5% CO_2 for 24 hours.

Effector cells

24 hours after plating the target cells, $2x10^6$ HEK 293T cells were plated in a volume of 10 ml 10% (v/v) supplemented DMEM plate of 100 mm diameters (p100).

Transfection

Target cells in the pilot assay:

24 hours after plating the target cells, cells were transfected with Renilla Luciferase and Firefly Luciferase under the control of the T7 promoter by JetPEI, according to the manufacturer's protocol. Cells were incubated in 10% supplemented DMEM during 48 hours.

Target cells in further cell-cell fusion assays:

24 hours after plating the target cells, these were transfected with increasing amounts of CCR5 (0.5 μg – 2 μg). The positive control cells (HEK 293 CD4 cells) were transfected with

the empty vector pcDNA3). All cells were transfected by Renilla Luciferase and Firefly Luciferase under the control of the T7 promoter. Transfection was done by JetPEI, according to the manufacturer's protocol. Cells were incubated in 10% supplemented DMEM during 48 hours.

Effector cells

24 hours after plating the effector cells, the envelope protein containing T-tropic gp120 (IIIB) and T7 polymerase were introduced into these cells by infection with recombinant vaccinia virus (vv-env-1) containing gp120, 8 µl virus/ $5x10^5$ cells. Cells were then incubated in 2% supplemented DMEM and 100 µg/ml rifampicine during 24 hours.

Fusion

After 24 hours incubation of the effector cells, these cells were lifted using 0.02% EDTA, washed and centrifuged at 1200 rpm for 5 minutes, before they were added to each well of the target cells in the p24w, 10^5 cells per well in a total volume of 500 µl 10% supplemented DMEM and 100µg/ml rifampicine, and left to incubate for 6 hours at 37°C. After incubation, the medium was removed, and the cells were left at -20°C overnight.

Measurement

Using the commercial kit Dual Glo® Luciferase Assay System (Promega), 200 µl of 20% (v/v) lysis buffer (25 mM Tris-phosphate (pH 7.8), 1% (v/v) Triton X-100, 1 mM EDTA, 1 mM DTT, 8 mM $MgCl_2$, 15% (v/v) glycerol) diluted in sterile water was added to each well, and the cells were left to incubate for 20 minutes in room temperature with gentle agitation. The lysates were then collected and 20 µl of each lysate was added to white luminate plates of 96 wells, quadruplicated. The Firefly Luciferase substrate reagent was then added, 20 µl per point, and Firefly Luciferase luminescence was immediately measured without filtrating the light. The Renilla Luciferase substrate reagent was then added, 20 µl per point, and Renilla Luciferase luminescence was immediately measured, filtrating the light at 486 nm. Measurements were done by the fluorimetre Wallac Envision 2104 Multilabel Reader.

Normalized Firefly/Renilla Luciferase ratios for each point were calculated, and relative ratios were finally calculated (Section 1.3.3).

2.11 Internalization Assay

$2x10^5$ cells were resuspended in 6 ml of depletion medium (0.1% (v/v) BSA and 10 mM HEPES). 1 ml was added to six 1.5 ml Eppendorf tubes. 100 nM CCL5 was added to each Eppendorf tube and incubation was performed at 37ºC with constant shaking. Aliquots (the content of 1 tube) were withdrawn at 0 min, 1 min, 5 min, 15 min, 30 min and 60 min, and the reaction was stopped by adding 1 ml cold PBS (4ºC) to each Eppendorf tube. Cells were then washed with PBS at 4ºC and centrifuged at 1200 rpm for 5 minutes. Samples from each incubation time were placed in transparent plates of 96 wells with v-shaped bottoms. Receptor levels of CCR5, CD4 and CXCR4 were determined by Flow Cytometry staining (Section 2.6), using specific monoclonal antibodies against CCR5, CD4 and CXCR4 in the cytometer Coulter Epics XL-MCL

RESULTS

It is better to understand a little than to misunderstand a lot.

-Anatole France

3.1 Receptor expression patterns and functionality of cells containing receptors fused with fluorescent proteins.

Prior to evaluation of receptor homo- and heterodimerization, the functionality of cells transfected with a fluorescent fusion receptor was assessed. HEK 293T cells were transiently transfected with CCR5 CFP and CXCR4 CFP (Section 2.4) and their expression detected by flow Cytometry staining (Section 2.6) (Fig. 3.1) and confirmed by confocal microscopy (Fig. 3.2)

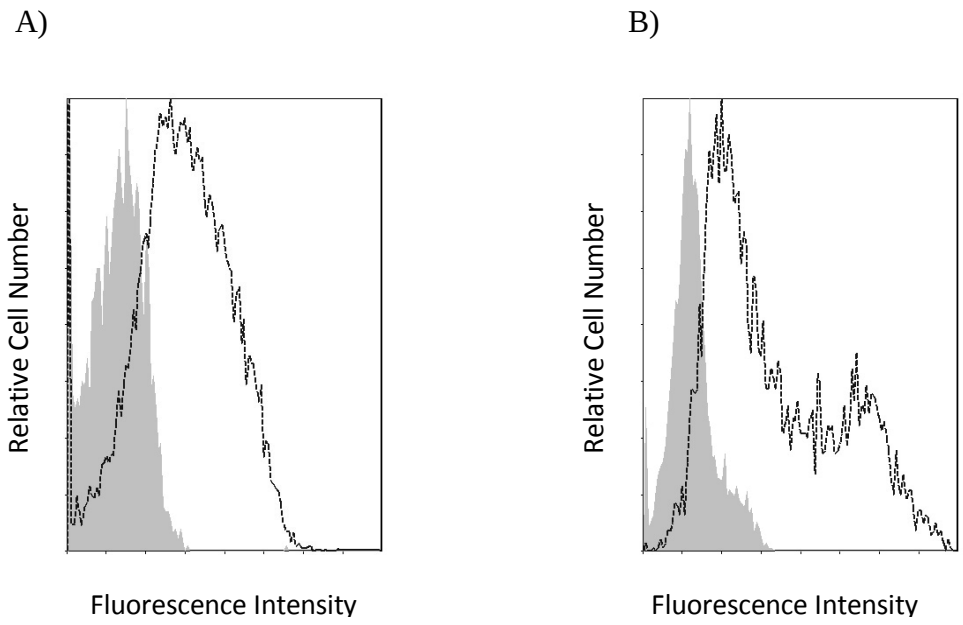

Figure 3.1: Representative staining results of A) CCR5 CFP, marked with monoclonal antibody IgG1 conjugated with SPRD. B) CXCR4 YFP, marked with monoclonal antibody IgG2A conjugated with FITC. Gray peaks represent the isotypes and the striped peaks represent the fluorochrome conjugated receptors.

A) *B)*

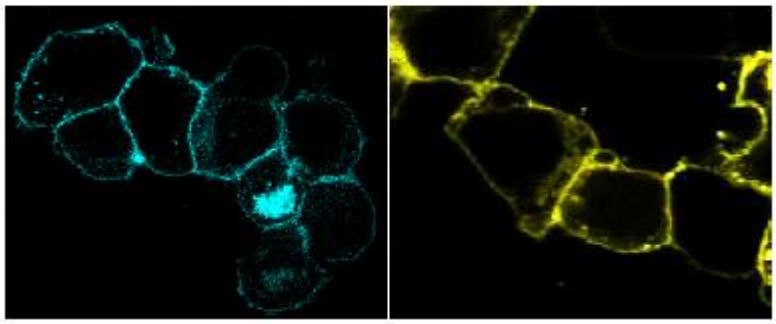

Figure 3.2: Representative images of A) CCR5-CFP and B) CXCR4-YFP by confocal microscopy. The images show that both CCR5 and CXCR4 are expressed at the cell surface, as well as intracellularily.

Functionality was then evaluated by a calcium flux assay (Section 2.5). HEK 293T cells transiently transfected with CCR5-CFP and HEK 293T cells transiently transfected with CXCR4-CFP responded normally to stimuli of CCL5 (50 nM) and CXCL12 (50 nM), respectively (Fig. 3.3), producing an equal response as the corresponding wildtype receptors upon ligand stimulation. All together, these data indicated that both receptors coupled to fluorescent molecules were fully functional and expressed correctly at the cell surface. Hence, they appear undistinguishable from wildtype receptors in terms of expression pattern and important activities.

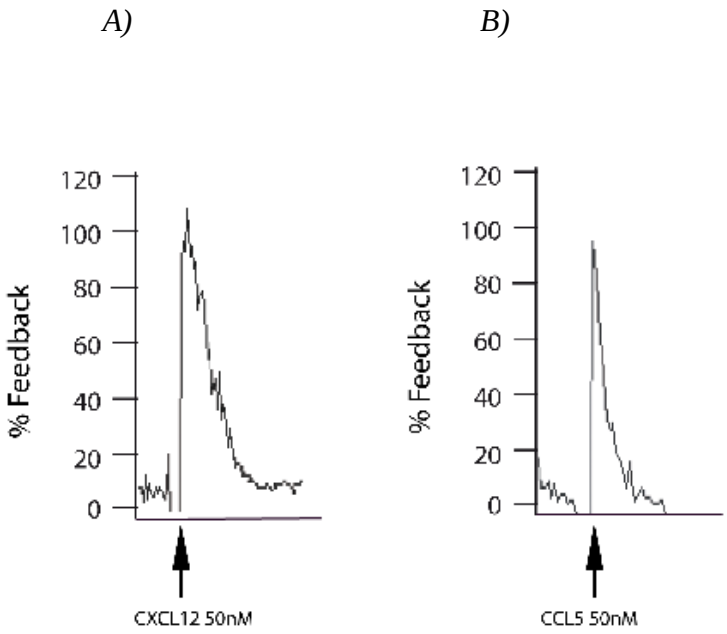

Figure 3.3: Calcium flux of A) CXCR4 with 50 nM CXCL12 and B) CCR5 with 50 nM CCL5. Both receptors respond normally to stimulation by their respective ligands.

3.2 Receptor Homo- and Heterodimerization

FRET techniques were used to analyze dimerization of CCR5 and CXCR4. To detect homo- and heterodimers in live cells, FRET saturation curves using HEK 293T cells transiently transfected with constant amounts of the donor protein (CFP-coupled CCR5 or CXCR4) and increasing amounts of the acceptor protein (YFP-coupled CCR5 or CXCR4) were generated (Section 2.7) Positive FRET was observed for both homodimers of CXCR4 and CCR5, and also for the heterodimer CCR5/CXCR4 (Fig. 3.4). Both homodimers showed differences in $FRET_{max}$ values (X4/X4, 0.7418 ± 0.0159; R5/R5, 0.51 ± 0.0517), but similar $FRET_{50}$ values (X4/X4, 0.5245 ± 0.0348; R5/R5 0.6693 ± 0.1574). The FRET results for the CCR5/CXCR4 heterodimer ($FRET_{max}$ 0.8229 ± 0.0958, $FRET_{50}$ 2.904 ± 0.671) indicated higher affinity of both receptors to form homodimers, rather than heterodimers. In the negative controls (CXCR4 CFP / the metatropic glutamate receptor conjugated to YFP and CCR5 CFP / the metatropic glutamate receptor conjugated to YFP) no FRET was observed (Fig. 3.5). This indicates specificity of the molecular interaction between the chemokine receptors. These data also demonstrate that $FRET_{max}$ was detected in cells at ≈ 1:1 YFP/CFP ratio.

To confirm the results of heterodimerization from the saturation curves, HEK 293T cells were transiently transfected with amounts of CCR5 CFP and CXCR4 YFP corresponding to an YFP/CFP ratio of 1:1. FRET was then determined by the acceptor photobleaching method (Section 2.8) and confocal microscopy. The results showed a FRET intensity of 15.2% ± 3.9 (Fig. 3.6)

A)

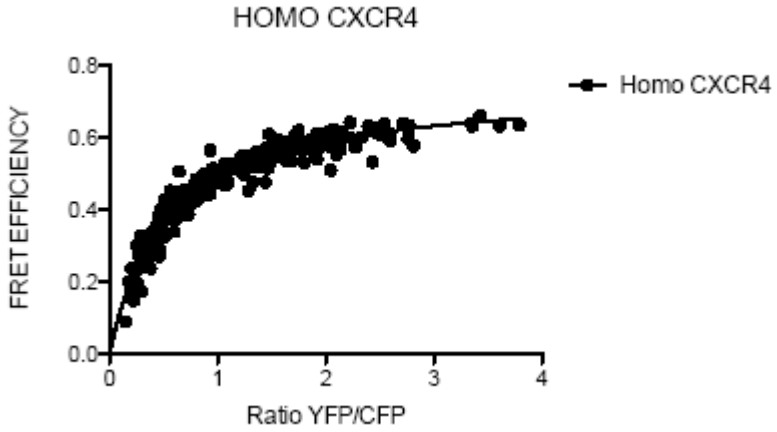

B)

	Values (95 % Confidence Intervals)
$FRET_{max}$	0.7418 ± 0.0159
$FRET_{50}$	0.5245 ± 0.0348

C)

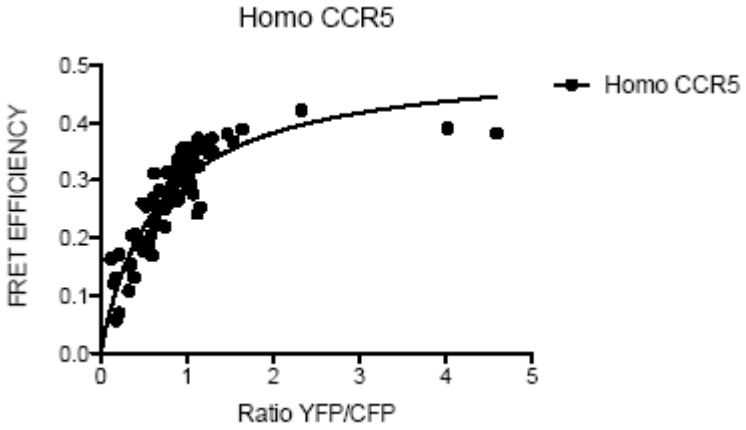

D)

	Values (95 % confidence intervals)
$FRET_{max}$	0.51 ± 0.0517
$FRET_{50}$	0.6693 ± 0.1574

E)

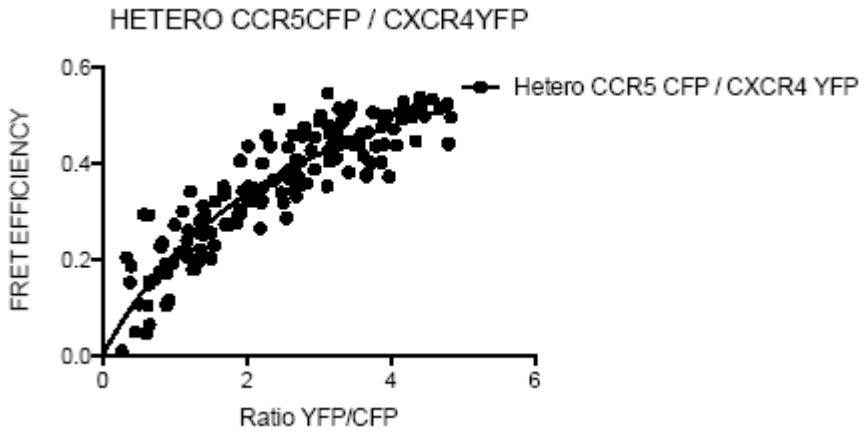

F)

	Values (95 % confidence intervals)
$FRET_{max}$	0.8229 ± 0.0958
$FRET_{50}$	2.904 ± 0.671

Figure 3.4: Saturation Curve of A) Homodimer CXCR4; C) Homodimer CCR5; E) Heterodimer CCR5 CFP/CXCR4 YFP; Values of $FRET_{max}$ and $FRET_{50}$ with 95% confidence intervals of B) Homodimer CXCR4; D) Homodimer CCR5; F) Heterodimer CCR5 CFP/CXCR4 YFP.

A)

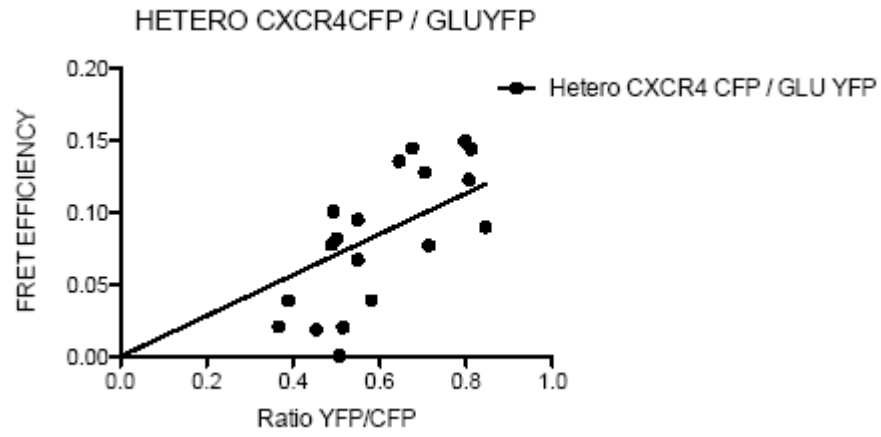

B)

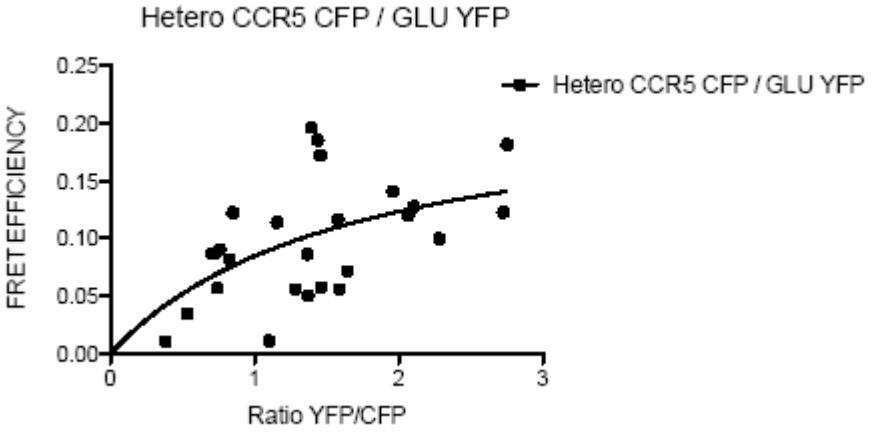

Figure 3.5: Saturation Curve of A) The heterodimer of CXCR4 CFP / the metatropic glutamate receptor conjugated to YFP; B) The heterodimer of CCR5 CFP / the metatropic glutamate receptor conjugated to YFP. Neither CXCR4 nor CCR5 form heterodimers with the metatropic glutamate receptor and these saturation curves hence serve as negative controls.

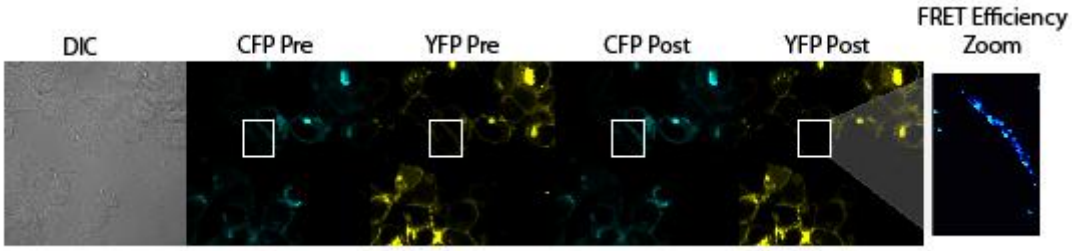

Figure 3.6: Representative images of FRET between CCR5CFP and CXCR4YFP, using confocal microscopy and the photobleaching method. The square in the middle shows the area of bleaching of YFP.

4.3 Receptor expression modulates receptor homo-and heterodimers

HEK 293T cells were transiently transfected with constant concentrations of CXCR4 CFP and increasing CXCR4 YFP concentrations in the presence of 9 µg CCR5 DNA. The receptor levels of CCR5 were established by flow Cytometry staining (Section 2.6) (Fig. 3.7) FRET saturation curves of the homodimer CXCR4CFP/CXCR4YFP in the presence of CCR5 were then evaluated. These resulted in a $FRET_{max}$ value of 0.8496 ± 0.0244 and a $FRET_{50}$ value 1.131 ± 0.098 (Fig. 3.8). CCR5 co-expression hence induced a statistical difference in the $FRET_{50}$ value, suggesting that CCR5 alters CXCR4 homodimerization. All together, these results indicate that receptor expression modulates CCR5 and CXCR4 conformations at the cell surface.

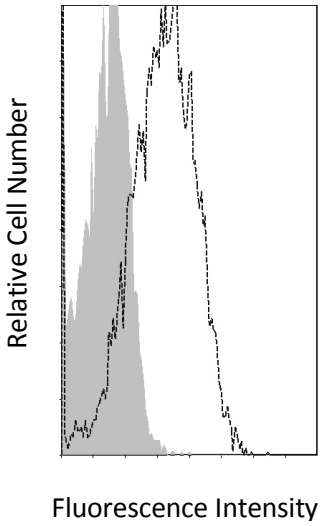

Figure 3.7: Representative staining of receptor levels of CCR5 in the cells of the saturation curve of CXCR4 + CCR5. The gray peak represents the isotype, and the striped peak represents the level of CCR5.

A)

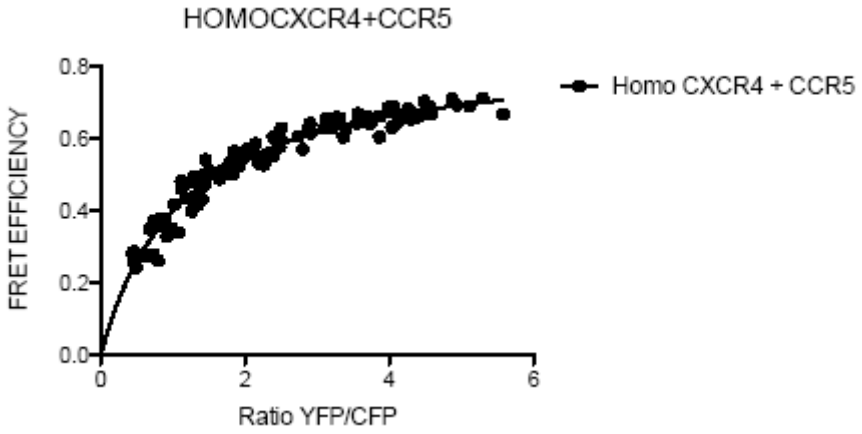

B)

	Values (95 % confidence intervals)
$FRET_{max}$	0.8496 ± 0.0244
$FRET_{50}$	1.131 ± 0.098

Figure 3.8: A) Saturation Curve of homo CXCR4 + CCR5. B) Values and 95 % confidence intervals of $FRET_{max}$ and $FRET_{50}$.

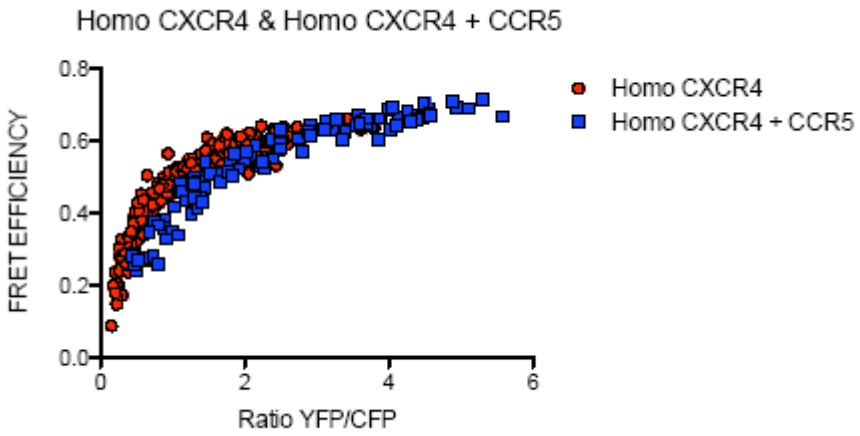

Figure 3.9: Saturation Curves of homo CXCR4 and homo CXCR4 + CCR5 put together in one graph.

4.4 CCR5 co-expression reduces T- tropic HIV- 1 viral infection

A possible modulation of the ability of T-tropic HIV-1 to infect the cells by dynamic regulation of CXCR4 homodimers by CCR5 co-expression was then assessed. To evaluate the CCR5 effect on T-Tropic HIV-1 viral entry, a pilot experiment was designed, using stable HEK 293 cells expressing CD4 and CXCR4, comparing these with other stable HEK 293 cell lines, co-expressing CD4, CXCR4 and CCR5. The levels of all three receptors were determined in all four cell lines by flow Cytometry staining (Section 2.6) using specific monoclonal antibodies against CCR5, CXCR4 and CD4 (Fig. 3.10). Cell-cell fusion assays (2.10) were performed using these cell lines as target cells and HEK 293T cells infected with recombinant vaccinia virus expressing the T-tropic envelope protein gp120 (IIIB) as effector cells. The infection levels detected in the cell lines expressing CD4 and CXCR4 was drastically reduced in cells expressing CCR5 (Fig. 3.11), indicating that CCR5 reduces T-tropic HIV-1 infection. However, as the level of CD4 receptors at the cell surface of both cell lines containing CCR5 differed from the cells expressing only CD4 and CXCR4, another strategy was established, in order to assure the role of CCR5 in the decrease of infection. HEK 293 cells stably expressing CD4 and CXCR4 were transiently transfected with increasing amounts of CCR5 (0.5 µg – 2.0 µg). The expression levels of all three receptors were determined by flow Cytometry staining (Section 2.6) using specific monoclonal

antibodies against CCR5, CXCR4 and CD4 (Fig. 3.12), and cell-cell fusion experiments were performed. These experiments clearly showed a correlation between reduction of infection and the levels of CCR5 expressed at the cell membrane (Figs. 3.13 and 3.14). The results thus indicated that CCR5 co-expression modulates CXCR4 homodimers at the cell surface, and reduces the ability of virus expressing T-tropic gp120 envelope proteins to infect the cell.

To confirm these data, the same cell-cell fusion experiments were performed in cells treated and untreated with CCL5, the specific ligand of CCR5, hence provoking internalization of this receptor (Section 2.11). A pilot experiment in order to determine the amount of CCL5 needed to detect internalization by flow Cytometry was performed, and it was found that incubating the cells with 100 nM CCL5 for 60 minutes at 37°C caused an internalization of 48.3%. Receptor levels of CD4 and CXCR4 were maintained at the cell surface (Fig. 3.15). HEK 293 cells stably expressing CD4 and CXCR4 were then transiently transfected with increasing amounts of CCR5 (0.5 μg – 2.0 μg) and treated with 100 nM CCL5 for 60 minutes at 37 °C. The expression levels of all three receptors were determined by flow Cytometry staining using specific monoclonal antibodies against CCR5, CXCR4 and CD4 (Section 2.6), and cell-cell fusion experiments were performed (Section 2.10). Flow Cytometry staining results showed an internalization of CCR5 of about 50% (Fig. 3.16). Receptor levels of CD4 and CXCR4 were maintained at the cell surface (not showed). Cell-cell fusion results showed that infection levels in cells treated with CCL5 were restored to the infection level of cells without CCR5 (Figs. 3.17 and 3.18).

All together, these results indicate that membrane expression of CCR5 modulate the conformations of CXCR4 and hence reduces the ability of T-tropic HIV-1 to infect the cell.

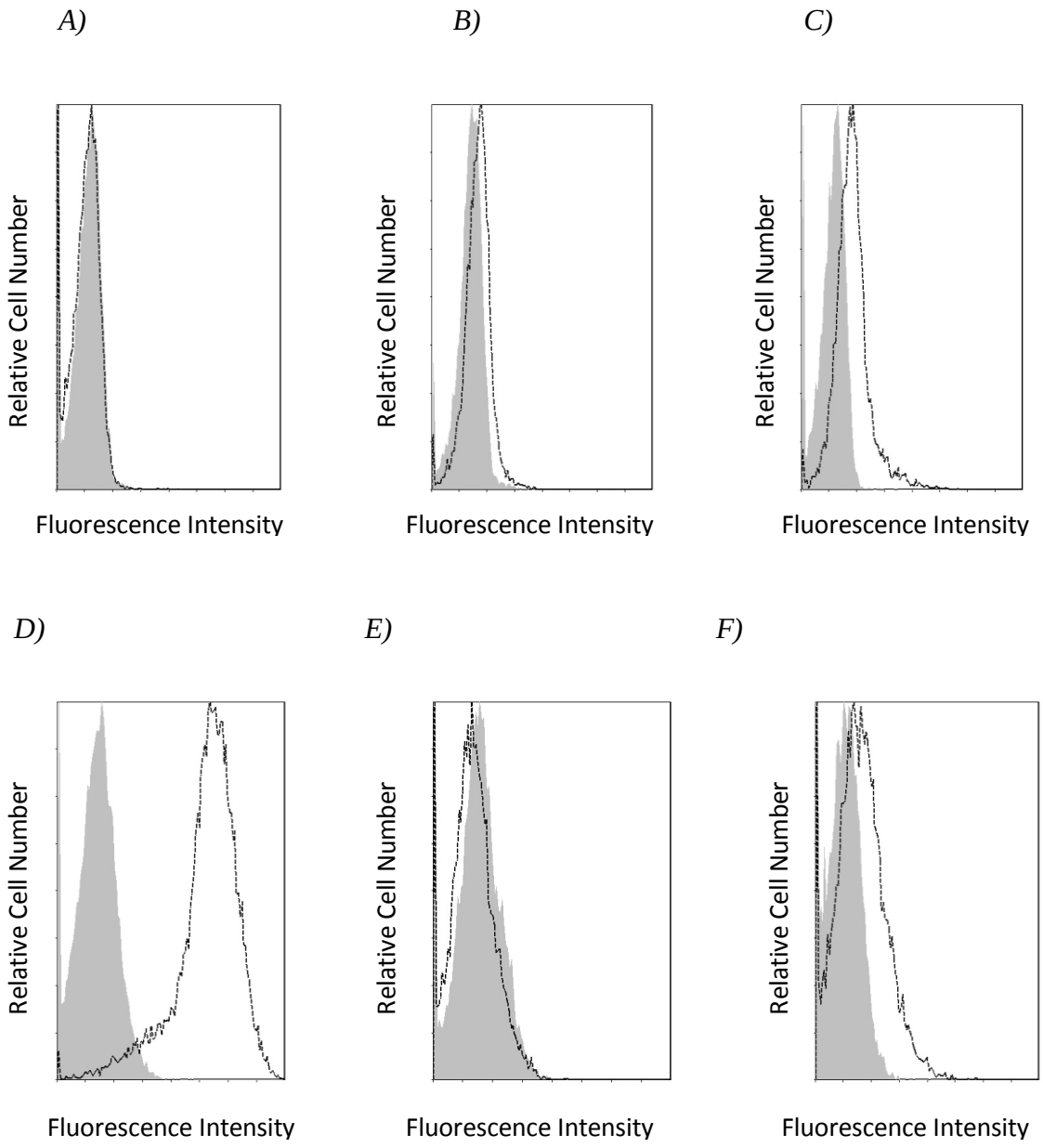
A)
B)
C)
Relative Cell Number
Fluorescence Intensity
D)
E)
F)

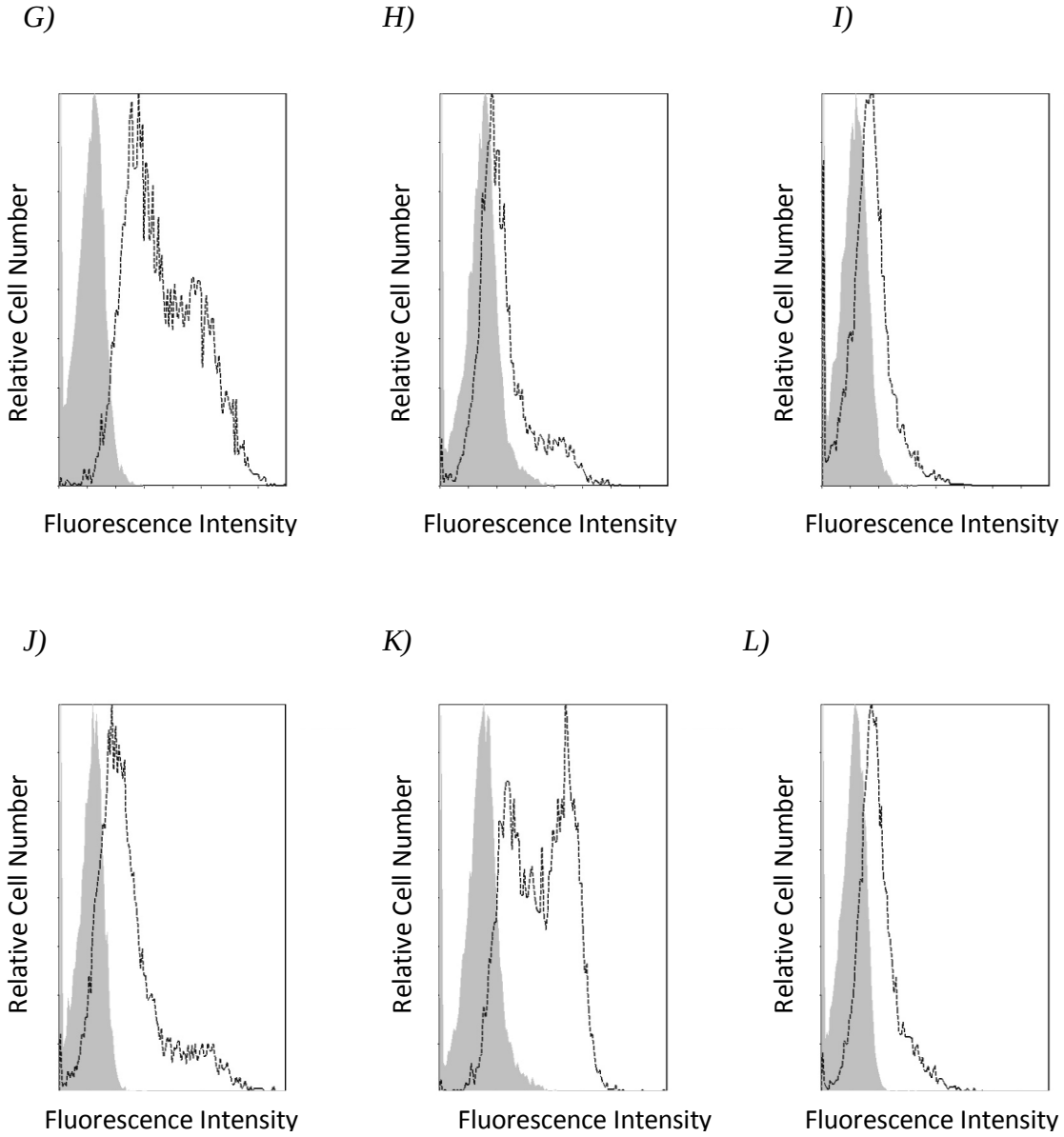

Figure 3.10: Receptor levels of A), D), G), J) CD4; B), E), H), K) CCR5; and C), F), I), L) CXCR4 of the four cell lines A), B), C) 293T Italy; D), F), G) 293 CD4; G), H), I) 293 CD4 (1.5 μg CCR5); and J), K), L) 293 CD4 (5.0 μg CCR5). Gray peaks represent the isotypes and the striped peaks represent the fluorochrome conjugated receptors. All cell lines express CXCR4 endogenously. 293 T Italy cells lack both CD4 and CCR5, and can therefore serve as a negative control for cell-cell fusion experiments. 293 CD4 cells express high amounts of CD4 stably, but lack CCR5.This cell line is therefore a positive control for cell-cell fusion experiments. 293 CD4 (1.5 μg CCR5) cells express CD4 and modest amounts of CCR5 stably, while 293 CD4 (5.0 μg CCR5) cells express CD4 and higher amounts of CCR5 stably.

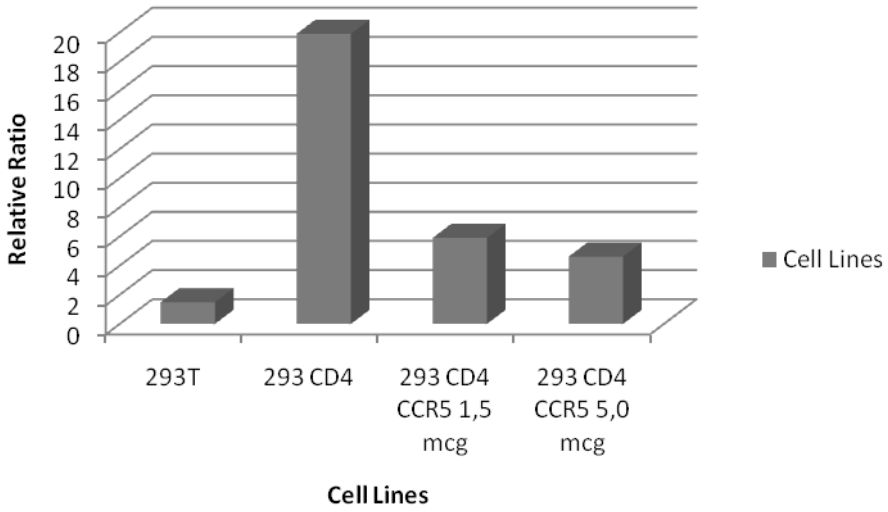

Figure 3.11: A representative cell-cell fusion experiment showing the relative ratios of different cell lines upon fusion with effector cells. A clear decrease of infection can be seen, as the relative ratio changes from ca. 20 in the cells only expressing CD4 and CXCR4, to ca. 4 in the cells expressing CCR5 in addition to CD4 and CXCR4.

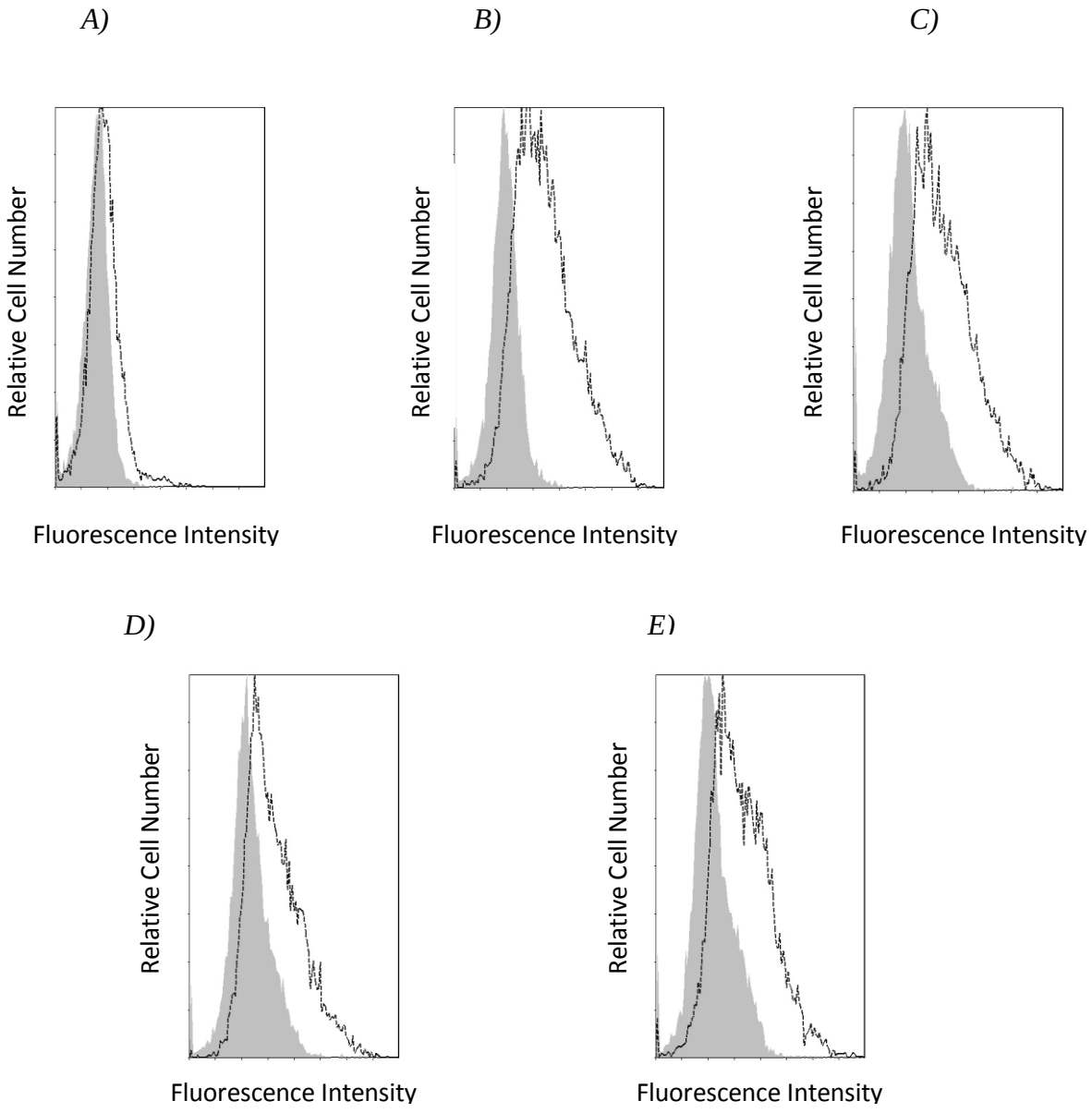
A)
B)
C)
Relative Cell Number
Fluorescence Intensity
Relative Cell Number
Fluorescence Intensity
Relative Cell Number
Fluorescence Intensity
D)
E)
Relative Cell Number
Fluorescence Intensity
Relative Cell Number
Fluorescence Intensity

F)

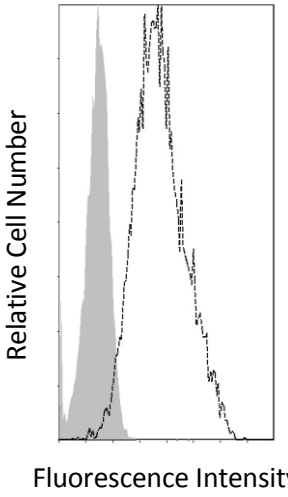
Relative Cell Number
Fluorescence Intensity

G)

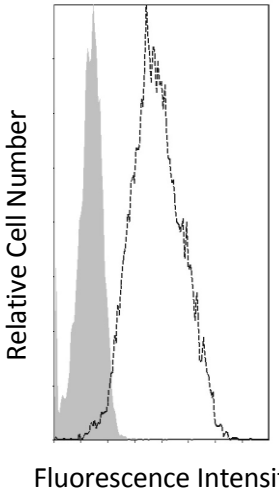
Relative Cell Number
Fluorescence Intensity

H)

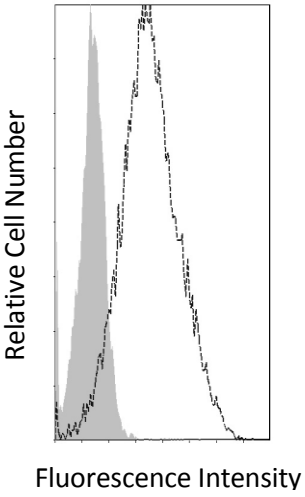
Relative Cell Number
Fluorescence Intensity

I)

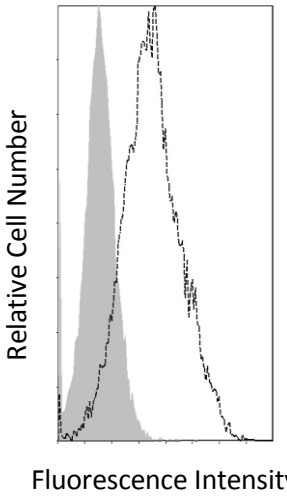
Relative Cell Number
Fluorescence Intensity

J)

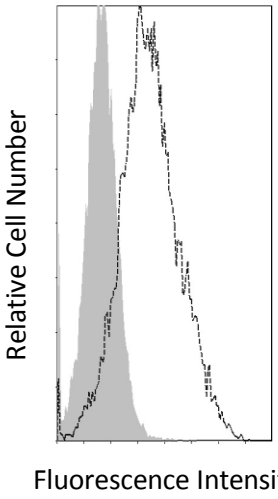
Relative Cell Number
Fluorescence Intensity

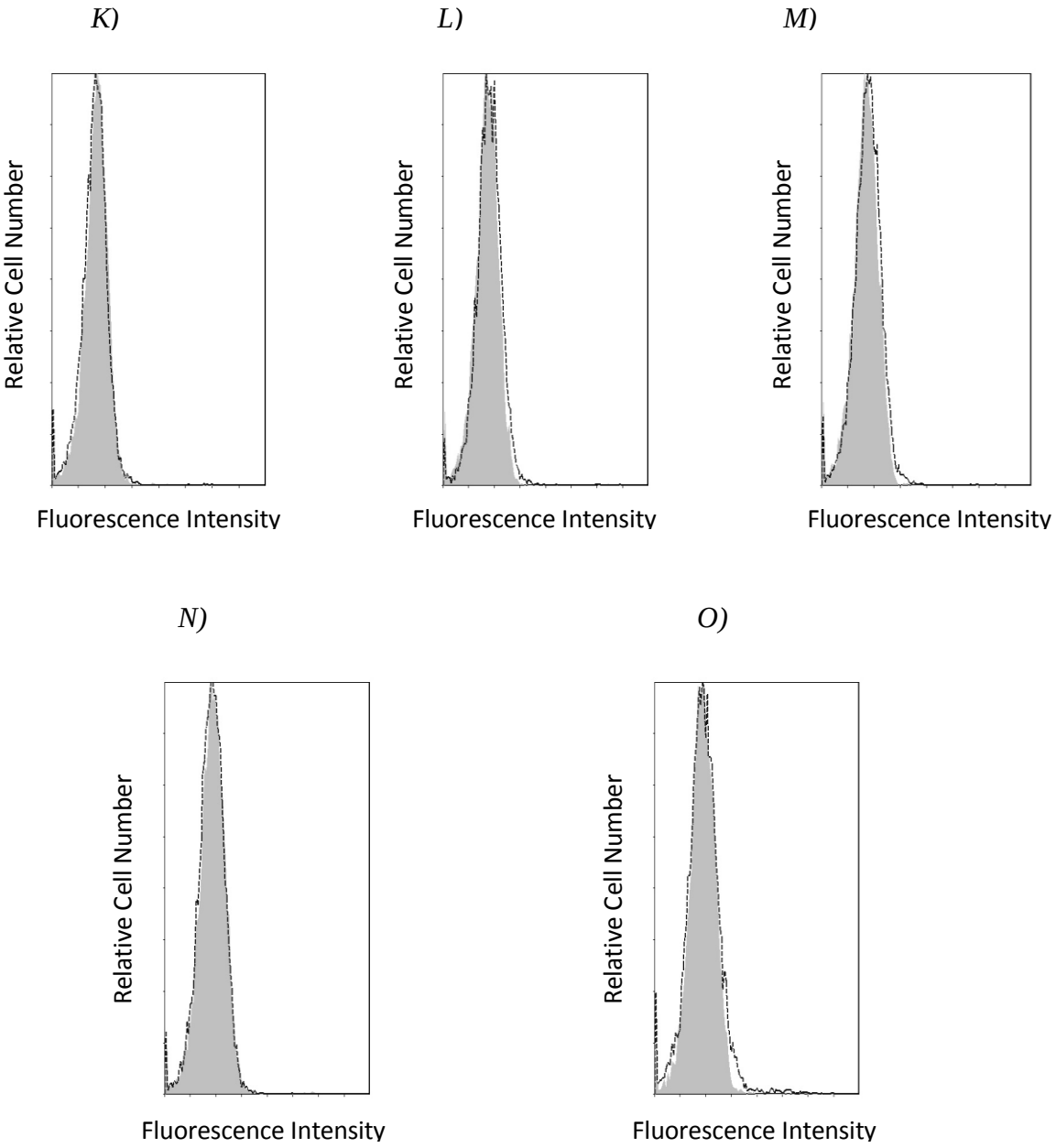

Figure 3.12: Receptor levels of A), B), C), D), E) CD4; F), G), H), I), J) CCR5; and K), L), M, N), O) CXCR4; at A), F), K) 2.0 μg empty vector pcDNA3; B), G), L), 0.5 μg CCR5; C), H), M) 1.0 μg CCR5; D), I), N) 1.5 μg CCR5, E) J), O) 2.0 μg CCR5. Gray peaks represent the isotypes and the striped peaks represent the fluorochrome conjugated receptors.

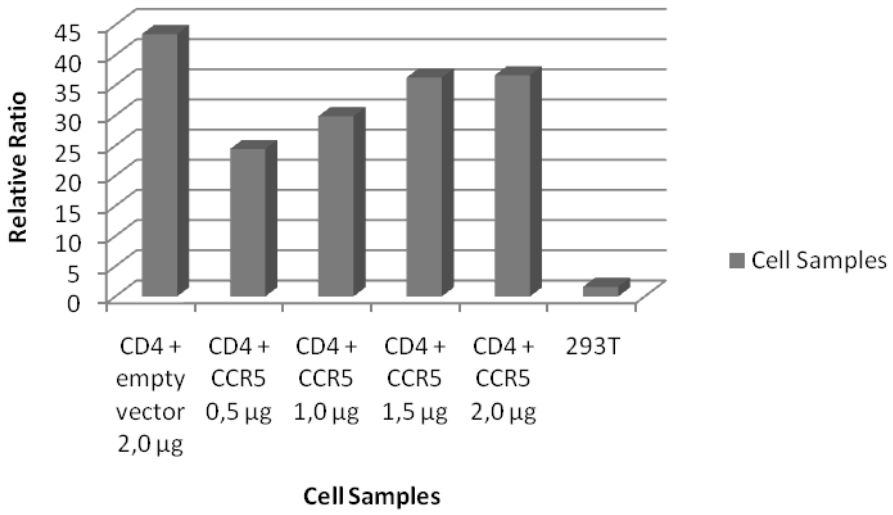

Figure 3.13: A representative cell-cell fusion experiment showing the relative ratios of 293 CD4 cells transiently transfected with increasing concentrations of CCR5, upon fusion with effector cells. As transfection of CCR5 increases (Fig. 3.14), infection levels decrease.

Percentage of transfection CCR5 (%)	
CD4 + CCR5 0.5 µg	40.92
CD4 + CCR5 1.0 µg	23.37
CD4 + CCR5 1.5 µg	14.04
CD4 + CCR5 2.0 µg	15.06

Figure 3.14: Receptor levels of the 293 CD4 cells in the cell-cell fusion assay (Fig. 3.13)

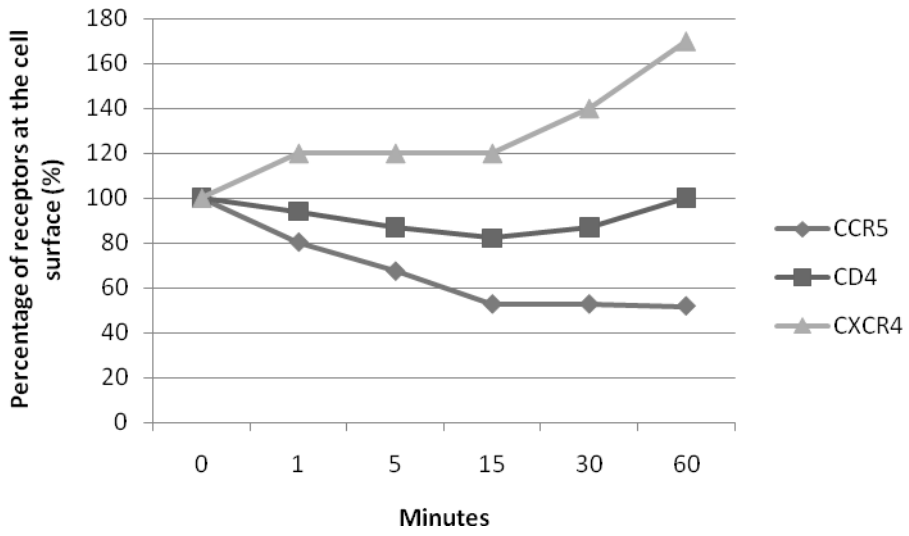

Figure 3.15: Representative experiment of internalization of CCR5 by stimulation with 100 nM CCL5. Receptor levels of CCR5, CD4 and CXCR4 at 0 min, 1 min, 5 min, 15 min, 30min and 60 min of incubation with CCL5at the cell surface. CCR5 internalizes, while CD4 and CXCR4 receptor levels are maintained at the cell surface.

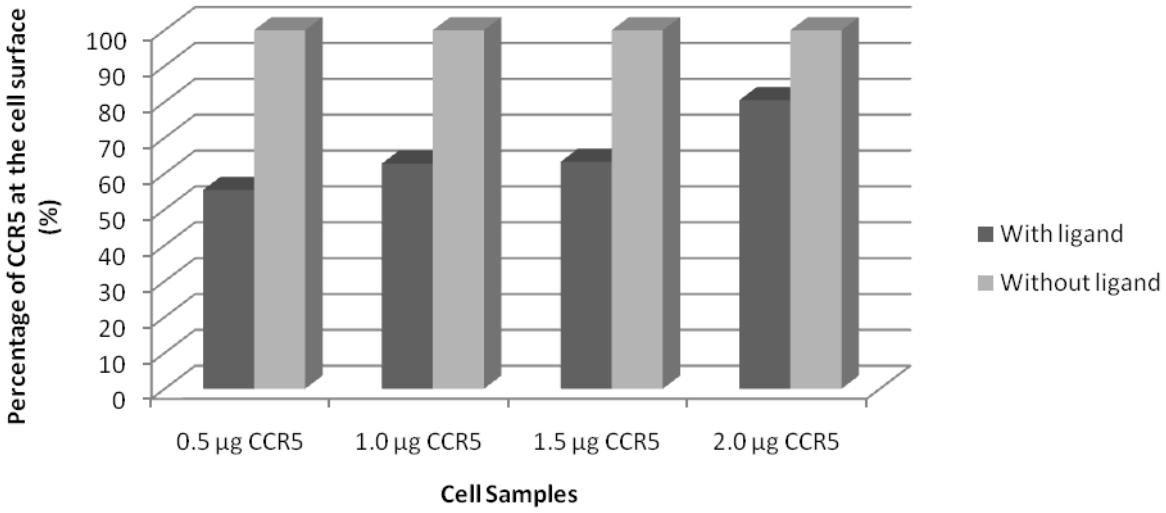

Figure 3.16: Representative experiment of internalization of CCR5 upon stimulating HEK 293 CD4 cells transiently transfected with increasing concentrations of CCR5 (0.5 – 2.0 µg) with CCL5 for 60 minutes. CCR5 internalizes to about 50% in cells transfected with 0.5 µg CCR5.

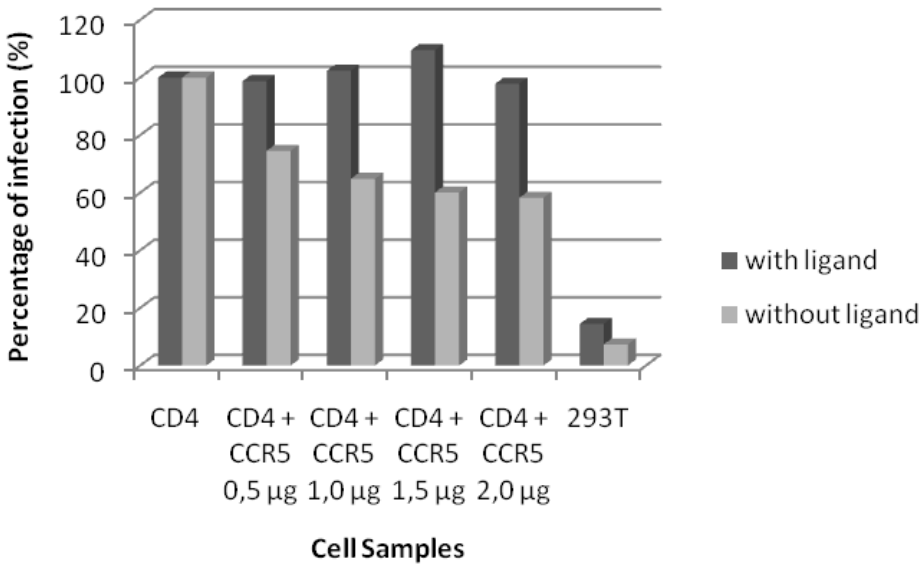

Figure 3.17: A representative cell-cell fusion experiment showing percentage of infection in cells treated with 100 nM CCL5 (Fig. 3.16) and cells untreated with CCL5 (Fig. 3.18). Infection levels in cells treated with CCL5 is clearly restored to infection levels of cells without CCR5.

Cell Samples	Percentage of transfection CCR5 (%)
0.5 µg CCR5	27.66
1.0 µg CCR5	24.87
1.5 µg CCR5	22.02
2.0 µg CCR5	21.25

Figure 4.18: Transfection levels of CCR5 in cells used in the cell-cell fusion assay (Fig. 3.17).

DISCUSSION

Although monomeric GPCRs can activate heterotrimeric G-proteins [64], many reports show evidence of their assembly into dimeric complexes, and even oligomerization was recently demonstrated [65]. Chemokine receptors are not an exception, and several reports demonstrate the existence of homo- and heterodimers in the absence of ligands [34]. This is the case of CCR5 and CXCR4, the two co-receptors for HIV-1 infection.

In this project, the expression patterns of CCR5 and CXCR4 has been evaluated, in addition to the conformations that they can adopt at the cell surface, their dynamics and the effect of this on T-tropic HIV-1 infection. Cell functionality and receptor levels were evaluated by flow Cytometry.

The first experiments revealing that dimerization of GPCRs existed were based on immunoprecipitation and Western Blotting. The SDS-PAGE technique is based on the distinct migration behaviour of the proteins when an electric field is applied. This technique was combined with Western Blots, in which the use of specific monoclonal antibodies allows detection of specific proteins. The results showed proteins with a higher molecular mass than would be expected of the monomeric receptor, and the molecular mass corresponded to that of multiple equal receptors [65]. In the cases of receptors lacking a specific antibody, these were marked with epitopes at the extreme N-terminus, and identified by antibodies specific to this epitope. The use of bifunctional compounds, also called “crosslinkers”, (ex. DSS) also became a good option, as fixing the receptor complexes made the interactions more stable, and easily detectable [66]. These techniques are still in use, although they present some difficulties. They are not applicable for cells *in vivo*, the use of detergents to solubilise the membrane receptors could disturb detection, and the need for specific antibodies in order to immunoprecipitate the receptors can provide a problem. Nowadays, techniques based on biophysical aspects, like ex. Resonance Energy Transfer (RET), are considered more appropriate for this kind of experiments.

In this project, FRET techniques were used for the evaluation of protein/protein interactions on the cell surface. These techniques show energy transfer between two fluorescent proteins, if they are located sufficiently close and correctly oriented to each other, as is the case in an oligomeric complex. First, receptor expression patterns and receptor functionality upon

stimulation with the ligands of both CCR5 and CXCR4 were evaluated on cells transfected with CCR5 and CXCR4 coupled to CFP and YFP. Neither receptor expression patterns nor receptor functionality varied from the wildtype receptors. The FRET method of saturation curves was used to determine homo- and heterodimerization between CCR5 and CXCR4. In these curves, based on constant donor concentration and increasing acceptor concentrations, it was found that CXCR4 and CCR5 form homodimers and heterodimers. By analogy to BRET parameters, one can assume that if energy transfer reaches saturation and the curve is hyperbolic, $FRET_{50}$ values would allow estimation of the apparent affinities between the receptors involved. Based on this, it was concluded that both CCR5 and CXCR4 form homo- and heterodimeric complexes at the cell surface, and that the differences in $FRET_{50}$ values observed between the saturation curves of the homo- and heterodimers indicated that both receptors have higher affinity towards forming homodimers than forming heterodimers. Thus, these data concur with previous reports showing that these complexes exist in the absence of ligands and that the affinity to form homodimers is higher than that of forming heterodimers [34, 35].

Acceptor photobleaching FRET data also confirmed CXCR4/CCR5 heterodimerization at the cell membrane. Results from this technique also showed that CXCR4 located itself better than CCR5 in the cell membrane. Although $FRET_{max}$ values between two different homodimers cannot be compared due to their mathematical formulas, it is possible that the data obtained from the saturation curves are affected by the expression pattern of the receptors in question. Bearing in mind this, it is interesting that the $FRET_{max}$ value of CCR5 was indeed much lower than that of CXCR4.

The FRET results of the saturation curves of the homodimer CXCR4 in competition with CCR5 showed that co-expression of CCR5 decreased the apparent affinity of CXCR4 to form homodimers, as the $FRET_{50}$ value of the homodimer CXCR4 in presence of CCR5 increased significantly compared to the homodimer CXCR4 alone. This could mean that some CXCR4 receptors form heterodimers with CCR5, affecting the homodimeric conformations of CXCR4. These data hence indicated that chemokine receptor co-expression is sufficient to allow heterodimeric complex formation and that homo- and heterodimers coexist at the cell membrane in the absence of ligands. All together, the results showed that homo- and heterodimerization is a dynamic system, depending among other things on the receptors expression at the cell surface.

The central question at this point was whether the apparent effect of CCR5 on the CXCR4 homodimer could affect T-tropic HIV-1 infection. CCR5 and CXCR4 are the two main co-receptors for HIV-1 infection, and previous published evidence suggests that receptor dimerization can influence this. [67]. Evaluation of HIV-1 entry was done by the method of cell-cell fusion between effectors containing the vaccinia virus expressing the T-tropic gp120 and target cells expressing CD4 and CXCR4 in the absence and presence of CCR5. Firefly and Renilla Luciferases served as reporters of infection. Hence, advantage was taken of an *in vitro* assay, thus avoiding the use of the natural virus. The results showed a clear correlation between CCR5 expression and a decrease in T-tropic HIV-1 infection. Maintaining CD4 and CXCR4 levels unchanged at the cell surface while increasing the concentration of CCR5 discarded an unspecific effect and assured the role of CCR5 in the decrease of infection. To confirm these observations, cells co-expressing CD4, CXCR4 and CCR5 were treated with CCL5, the specific ligand of CCR5, and all three receptor levels were evaluated by Flow Cytometry. As expected, CCL5 induced the internalization of CCR5 without affecting the levels of CD4 and CXCR4 at the cell surface. Parallel cell-cell fusion of the CCL5 treated cells with effectors showed that infection levels were restored to the control levels in cells not expressing CCR5. CCL5 mediated downregulation of CCR5 was thus sufficient to restore the CXCR4 conformation allowing T-tropic HIV-1 entry and infection.

All together, these results suggest that the conformation dynamics of the main co-receptor of T-tropic HIV-1 in the presence of CCR5, can decrease the capacity of HIV-1 to enter the cell, and hence infection.

Future Perspectives

Currently, this research project opens new questions. As previous mentioned, HIV-1 infection requires the presence of CD4 and one of the co-receptors (CXCR4 or CCR5). Until now, only the ability of CCR5 to decrease the apparent affinity of CXCR4 homodimer conformation by heterodimerization, and hence alter further interaction between CXCR4 and CD4 has been studied. However, an alternative hypothesis could be that CCR5 also modulates CD4 conformations. Some reports suggest that CD4 interacts with both CCR5 and CXCR4 [68], and it is thus necessary to analyze this possibility, by for example generating saturation curves of the homodimer CD4/CD4 and the heterodimers CD4/CCR5 and CD4/CXCR4, comparing the apparent affinities between the different dimers. Another possibility is the formation of a

heterotrimeric complex between all three receptors (CD4, CCR5 and CXCR4) at the cell surface. If CXCR4 and CD4 are capable of forming heterodimers and gp120 binds to these receptors in this conformation, the sudden presence of CCR5 could possibly alter the conformation of these receptors, by forming heterodimers with either one of the receptors, or by joining the complex, forming a heterotrimer. In this last case, CCR5 may be capable of altering the position of CD4 and CXCR4 enough to block the correct binding of gp120. The possibility of a heterotrimeric complex can be assessed by the use of multicolour Bimolecular Fluorescence Complementation (BiFC). In this technique, CXCR4 for example, would be coupled to a so-called split YFP, consisting of a fragment of YFP (the N-terminal part of YFP), whereas CCR5 would be coupled to the complementary fragment (the C-terminal part of YFP), thus only allowing for YFP detection upon interaction between CXCR4 and CCR5. CD4 would then be coupled to CFP, and thus, positive FRET would be observed between all three receptors if these were to form an oligomeric complex.

During my project, it has become clear that CCR5 is capable of decreasing T-tropic HIV-1 infection through interaction with CXCR4, CD4 or both. The exact mechanism for this effect is yet to be determined by the techniques described above.

CONCLUDING REMARKS

- CXCR4 and CCR5 have been generated as CFP and YFP fusion proteins, and these proteins have been used to determine homo- and heterodimerization of CXCR4 and CCR5 at the cell surface.
- The expression patterns of CCR5-CFP and CXCR4-YFP do not differ from those of the wild type receptors.
- CCR5-CFP and CXCR4-CFP responded normally to the corresponding ligands (CCL5 and CXCL12, respectively) in terms of Ca^{2+} flux, indicating that they are fully functional.
- CCR5 and CXCR4 form homo-and heterodimers at the cell surface.
- Both homo- and heterodimers co-exist at the cell membrane in the absence of ligands.
- CCR5 co-expression reduces the apparent affinity of CXCR4 towards forming homodimers, indicating possible conformation changes of CXCR4 in the presence of CCR5.
- CCR5 and CXCR4 homo-and heterodimerization are dynamically regulated by receptor expression.
- T-tropic HIV-1 entry is reduced in cells co-expressing CCR5, in addition to CD4 and CXCR4, suggesting that CCR5/CXCR4 heterodimerization modulate T-tropic HIV-1 infection.

REFERENCES

1. Clore, G.M. and A.M. Gronenborn, *Three-dimensional structures of alpha and beta chemokines.* FASEB J, 1995. **9**(1): p. 57-62.
2. Nesmelova, I.V., et al., *CXC and CC chemokines form mixed heterodimers: association free energies from molecular dynamics simulations and experimental correlations.* J Biol Chem, 2008. **283**(35): p. 24155-66.
3. Zlotnik, A. and O. Yoshie, *Chemokines: a new classification system and their role in immunity.* Immunity, 2000. **12**(2): p. 121-7.
4. Allen, S.J., S.E. Crown, and T.M. Handel, *Chemokine: receptor structure, interactions, and antagonism.* Annu Rev Immunol, 2007. **25**: p. 787-820.
5. Hemmerich, S., et al., *Identification of residues in the monocyte chemotactic protein-1 that contact the MCP-1 receptor, CCR2.* Biochemistry, 1999. **38**(40): p. 13013-25.
6. Jarnagin, K., et al., *Identification of surface residues of the monocyte chemotactic protein 1 that affect signaling through the receptor CCR2.* Biochemistry, 1999. **38**(49): p. 16167-77.
7. Mizoue, L.S., et al., *Molecular determinants of receptor binding and signaling by the CX3C chemokine fractalkine.* J Biol Chem, 2001. **276**(36): p. 33906-14.
8. Signoret, N., et al., *Endocytosis and recycling of the HIV coreceptor CCR5.* J Cell Biol, 2000. **151**(6): p. 1281-94.
9. Crump, M.P., et al., *Solution structure and basis for functional activity of stromal cell-derived factor-1; dissociation of CXCR4 activation from binding and inhibition of HIV-1.* EMBO J, 1997. **16**(23): p. 6996-7007.
10. Lander, E.S., et al., *Initial sequencing and analysis of the human genome.* Nature, 2001. **409**(6822): p. 860-921.
11. Flower, D.R., *Modelling G-protein-coupled receptors for drug design.* Biochim Biophys Acta, 1999. **1422**(3): p. 207-34.
12. Fredriksson, R., et al., *The G-protein-coupled receptors in the human genome form five main families. Phylogenetic analysis, paralogon groups, and fingerprints.* Mol Pharmacol, 2003. **63**(6): p. 1256-72.
13. Mellado, M., et al., *The chemokine monocyte chemotactic protein 1 triggers Janus kinase 2 activation and tyrosine phosphorylation of the CCR2B receptor.* J Immunol, 1998. **161**(2): p. 805-13.
14. Palczewski, K., et al., *Crystal structure of rhodopsin: A G protein-coupled receptor.* Science, 2000. **289**(5480): p. 739-45.
15. Cherezov, V., et al., *High-resolution crystal structure of an engineered human beta2-adrenergic G protein-coupled receptor.* Science, 2007. **318**(5854): p. 1258-65.
16. Henderson, R., et al., *Model for the structure of bacteriorhodopsin based on high-resolution electron cryo-microscopy.* J Mol Biol, 1990. **213**(4): p. 899-929.
17. *Chemokine/chemokine receptor nomenclature.* Cytokine, 2003. **21**(1): p. 48-9.
18. Jiang, H., et al., *Pertussis toxin-sensitive activation of phospholipase C by the C5a and fMet-Leu-Phe receptors.* J Biol Chem, 1996. **271**(23): p. 13430-4.
19. Marte, B.M., et al., *R-Ras can activate the phosphoinositide 3-kinase but not the MAP kinase arm of the Ras effector pathways.* Curr Biol, 1997. **7**(1): p. 63-70.
20. Jones, S.A., B. Moser, and M. Thelen, *A comparison of post-receptor signal transduction events in Jurkat cells transfected with either IL-8R1 or IL-8R2. Chemokine mediated activation of p42/p44 MAP-kinase (ERK-2).* FEBS Lett, 1995. **364**(2): p. 211-4.

21. Blanpain, C., et al., *The core domain of chemokines binds CCR5 extracellular domains while their amino terminus interacts with the transmembrane helix bundle.* J Biol Chem, 2003. **278**(7): p. 5179-87.
22. Bannert, N., et al., *Sialylated O-glycans and sulfated tyrosines in the NH2-terminal domain of CC chemokine receptor 5 contribute to high affinity binding of chemokines.* J Exp Med, 2001. **194**(11): p. 1661-73.
23. Schwarz, M.K. and T.N. Wells, *New therapeutics that modulate chemokine networks.* Nat Rev Drug Discov, 2002. **1**(5): p. 347-58.
24. Agnati, L.F. and K. Fuxe, *On the mechanism of the antiparkinsonian action of 1-DOPA and bromocriptine: a theoretical and experimental analysis of dopamine receptor sub- and supersensitivity.* J Neural Transm Suppl, 1980(16): p. 69-81.
25. Franco, R., et al., *Evidence for adenosine/dopamine receptor interactions: indications for heteromerization.* Neuropsychopharmacology, 2000. **23**(4 Suppl): p. S50-9.
26. Chabre, M. and M. le Maire, *Monomeric G-protein-coupled receptor as a functional unit.* Biochemistry, 2005. **44**(27): p. 9395-403.
27. Gurevich, V.V. and E.V. Gurevich, *How and why do GPCRs dimerize?* Trends Pharmacol Sci, 2008. **29**(5): p. 234-40.
28. Terrillon, S., C. Barberis, and M. Bouvier, *Heterodimerization of V1a and V2 vasopressin receptors determines the interaction with beta-arrestin and their trafficking patterns.* Proc Natl Acad Sci U S A, 2004. **101**(6): p. 1548-53.
29. Salahpour, A., et al., *Homodimerization of the beta2-adrenergic receptor as a prerequisite for cell surface targeting.* J Biol Chem, 2004. **279**(32): p. 33390-7.
30. Hanson, S.M., et al., *Each rhodopsin molecule binds its own arrestin.* Proc Natl Acad Sci U S A, 2007. **104**(9): p. 3125-8.
31. Mellado, M., et al., *Chemokine control of HIV-1 infection.* Nature, 1999. **400**(6746): p. 723-4.
32. Babcock, G.J., M. Farzan, and J. Sodroski, *Ligand-independent dimerization of CXCR4, a principal HIV-1 coreceptor.* J Biol Chem, 2003. **278**(5): p. 3378-85.
33. Issafras, H., et al., *Constitutive agonist-independent CCR5 oligomerization and antibody-mediated clustering occurring at physiological levels of receptors.* J Biol Chem, 2002. **277**(38): p. 34666-73.
34. Mellado, M., et al., *Chemokine signaling and functional responses: the role of receptor dimerization and TK pathway activation.* Annu Rev Immunol, 2001. **19**: p. 397-421.
35. Percherancier, Y., et al., *Bioluminescence resonance energy transfer reveals ligand-induced conformational changes in CXCR4 homo- and heterodimers.* J Biol Chem, 2005. **280**(11): p. 9895-903.
36. de Juan, D., et al., *A framework for computational and experimental methods: identifying dimerization residues in CCR chemokine receptors.* Bioinformatics, 2005. **21 Suppl 2**: p. ii13-8.
37. Benkirane, M., et al., *Mechanism of transdominant inhibition of CCR5-mediated HIV-1 infection by ccr5delta32.* J Biol Chem, 1997. **272**(49): p. 30603-6.
38. Mellado, M., A.C. Martinez, and J.M. Rodriguez-Frade, *Analysis of G-protein-coupled receptor dimerization following chemokine signaling.* Methods, 2002. **27**(4): p. 349-57.
39. Sierro, F., et al., *Disrupted cardiac development but normal hematopoiesis in mice deficient in the second CXCL12/SDF-1 receptor, CXCR7.* Proc Natl Acad Sci U S A, 2007. **104**(37): p. 14759-64.
40. Sohy, D., M. Parmentier, and J.Y. Springael, *Allosteric transinhibition by specific antagonists in CCR2/CXCR4 heterodimers.* J Biol Chem, 2007. **282**(41): p. 30062-9.
41. Contento, R.L., et al., *CXCR4-CCR5: a couple modulating T cell functions.* Proc Natl Acad Sci U S A, 2008. **105**(29): p. 10101-6.

42. Isik, N., D. Hereld, and T. Jin, *Fluorescence resonance energy transfer imaging reveals that chemokine-binding modulates heterodimers of CXCR4 and CCR5 receptors.* PLoS One, 2008. **3**(10): p. e3424.
43. Sohy, D., et al., *Hetero-oligomerization of CCR2, CCR5, and CXCR4 and the protean effects of "selective" antagonists.* J Biol Chem, 2009. **284**(45): p. 31270-9.
44. Martinez Munoz, L., et al., *Dynamic regulation of CXCR1 and CXCR2 homo- and heterodimers.* J Immunol, 2009. **183**(11): p. 7337-46.
45. Zou, Y.R., et al., *Function of the chemokine receptor CXCR4 in haematopoiesis and in cerebellar development.* Nature, 1998. **393**(6685): p. 595-9.
46. Tachibana, K., et al., *The chemokine receptor CXCR4 is essential for vascularization of the gastrointestinal tract.* Nature, 1998. **393**(6685): p. 591-4.
47. Strieter, R.M., et al., *CXC chemokines in angiogenesis.* Cytokine Growth Factor Rev, 2005. **16**(6): p. 593-609.
48. Ribeiro, S. and R. Horuk, *The clinical potential of chemokine receptor antagonists.* Pharmacol Ther, 2005. **107**(1): p. 44-58.
49. Zhao, Q., *Dual targeting of CCR2 and CCR5: therapeutic potential for immunologic and cardiovascular diseases.* J Leukoc Biol.
50. Barnes, D.A., et al., *Polyclonal antibody directed against human RANTES ameliorates disease in the Lewis rat adjuvant-induced arthritis model.* J Clin Invest, 1998. **101**(12): p. 2910-9.
51. Gerard, C. and B.J. Rollins, *Chemokines and disease.* Nat Immunol, 2001. **2**(2): p. 108-15.
52. Solomon, M., B. Balasa, and N. Sarvetnick, *CCR2 and CCR5 chemokine receptors differentially influence the development of autoimmune diabetes in the NOD mouse.* Autoimmunity. **43**(2): p. 156-63.
53. Doranz, B.J., et al., *A dual-tropic primary HIV-1 isolate that uses fusin and the beta-chemokine receptors CKR-5, CKR-3, and CKR-2b as fusion cofactors.* Cell, 1996. **85**(7): p. 1149-58.
54. Berger, E.A., et al., *A new classification for HIV-1.* Nature, 1998. **391**(6664): p. 240.
55. Venkatesan, S., et al., *Reduced cell surface expression of CCR5 in CCR5Delta 32 heterozygotes is mediated by gene dosage, rather than by receptor sequestration.* J Biol Chem, 2002. **277**(3): p. 2287-301.
56. Baleux, F., et al., *A synthetic CD4-heparan sulfate glycoconjugate inhibits CCR5 and CXCR4 HIV-1 attachment and entry.* Nat Chem Biol, 2009. **5**(10): p. 743-8.
57. Watabe, T., et al., *Fold recognition of the human immunodeficiency virus type 1 V3 loop and flexibility of its crown structure during the course of adaptation to a host.* Genetics, 2006. **172**(3): p. 1385-96.
58. Cormier, E.G. and T. Dragic, *The crown and stem of the V3 loop play distinct roles in human immunodeficiency virus type 1 envelope glycoprotein interactions with the CCR5 coreceptor.* J Virol, 2002. **76**(17): p. 8953-7.
59. Kamp, C., *Understanding the HIV coreceptor switch from a dynamical perspective.* BMC Evol Biol, 2009. **9**: p. 274.
60. Centre,M.C.S.;Availablefrom: http://images.google.com/imgres?imgurl=http://flow.csc.mrc.ac.uk/wp-content/uploads/fcm-fig1-overview1.jpg&imgrefurl=http://flow.csc.mrc.ac.uk/%3Fpage_id%3D302&usg=__S2c3_3Vbw3KwcQGEUD5o6kgWVKE=&h=659&w=1020&sz=43&hl=no&start=1&itbs=1&tbnid=HbDLArstb8IDXM:&tbnh=97&tbnw=150&prev=/images%3Fq%3Dflow%2Bcytometry%2Binvitrogen%26hl%3Dno%26gbv%3D2%26tbs%3Disch:1.
61. Pfleger, K.D. and K.A. Eidne, *Monitoring the formation of dynamic G-protein-coupled receptor-protein complexes in living cells.* Biochem J, 2005. **385**(Pt 3): p. 625-37.
62. Zimmermann, T., et al., *Spectral imaging and linear un-mixing enables improved FRET efficiency with a novel GFP2-YFP FRET pair.* FEBS Lett, 2002. **531**(2): p. 245-9.

63. Rucker, J., et al., *Cell-cell fusion assay to study role of chemokine receptors in human immunodeficiency virus type 1 entry.* Methods Enzymol, 1997. **288**: p. 118-33.
64. Ernst, O.P., et al., *Monomeric G protein-coupled receptor rhodopsin in solution activates its G protein transducin at the diffusion limit.* Proc Natl Acad Sci U S A, 2007. **104**(26): p. 10859-64.
65. Salim, K., et al., *Oligomerization of G-protein-coupled receptors shown by selective co-immunoprecipitation.* J Biol Chem, 2002. **277**(18): p. 15482-5.
66. Rodriguez-Frade, J.M., et al., *The chemokine monocyte chemoattractant protein-1 induces functional responses through dimerization of its receptor CCR2.* Proc Natl Acad Sci U S A, 1999. **96**(7): p. 3628-33.
67. Rodriguez-Frade, J.M., et al., *Blocking HIV-1 infection via CCR5 and CXCR4 receptors by acting in trans on the CCR2 chemokine receptor.* Embo J, 2004. **23**(1): p. 66-76.
68. Xiao, X., et al., *Constitutive cell surface association between CD4 and CCR5.* Proc Natl Acad Sci U S A, 1999. **96**(13): p. 7496-501.